64-12

FDL TDR 64-4

EXPERIMENTAL STUDIES OF HIGH TEMPERATURE HYPERSONIC DIFFUSERS

RICHARD T. SMITH

TECHNICAL DOCUMENTARY REPORT No. FDL TDR 64-4

FEBRUARY 1964

AF FLIGHT DYNAMICS LABORATORY
RESEARCH AND TECHNOLOGY DIVISION
AIR FORCE SYSTEMS COMMAND
WRIGHT-PATTERSON AIR FORCE BASE, OHIO

Project No. 1426, Task No. 142612

NOTICES

When Government drawings, specifications, or other data are used for any purpose other than in connection with a definitely related Government procurement operation, the United States Government thereby incurs no responsibility nor any obligation whatsoever; and the fact that the Government may have formulated, furnished, or in any way supplied the said drawings, specifications, or other data, is not to be regarded by implication or otherwise as in any manner licensing the holder or any other person or corporation, or conveying any rights or permission to manufacture, use, or sell any patented invention that may in any way be related thereto.

Qualified requesters may obtain copies of this report from the Defense Documentation Center (DDC), (formerly ASTIA), Cameron Station, Bldg. 5, 5010 Duke Street, Alexandria, Virginia, 22314.

This report has been released to the Office of Technical Services, U.S. Department of Commerce, Washington 25, D. C., in stock quantities for sale to the general public.

Copies of this report should not be returned to the Research and Technology Division, Wright-Patterson Air Force Base, Ohio, unless return is required by security considerations, contractual obligations, or notice on a specific document.

300 - April 1964 - 162 - 35-673

FOREWORD

This report was prepared by Richard T. Smith of the Electrogasdynamics Test Branch, AF Flight Dynamics Laboratory, Research and Technology Division, Wright-Patterson Air Force Base, Ohio. It presents the results of hypersonic gasdynamic tests of high temperature hypersonic diffusers during Sep-Dec 1963.

A search was made for diffuser data applicable to the Fifty-Megawatt Electrogasdynamic Facility. Finding no data available in the high temperature range (4000° R-12,000° R), an in-house study was initiated by Mr. Demetrius Zonars, Assitant to the Chief of the Flight Mechanics Division.

The author is pleased to acknowledge the helpful comments and technical guidance of Mr. D. Zonars and Mr. Franz J. A. Huber of the Electrogasdynamics Test Branch.

ABSTRACT

The effect of various diffuser configurations and blunted cone models on tunnel blockage and pressure recovery of a high temperature hypersonic gasdynamics facility is presented. These studies were conducted in the RTD One-Megawatt Prototype Electrogasdynamic Facility operating continuously with dry air. All data were obtained with frozen flow at Mach number 7.6, a stagnation enthalpy of 3000 BTU/lb, and an arc chamber pressure of 7 atmospheres. To determine the effects of extreme air temperatures, the total enthalpy was varied to 6000 BTU/lb with one diffuser configuration.

This technical documentary report has been reviewed and is approved.

P. P. ANTONATOS
Chief, Flight Mechanics Division
AF Flight Dynamics Laboratory

TABLE OF CONTENTS

ILLUSTRATIONS (CONT'D)

SYMBOLS

P_o	arc chamber stagnation pressure, atmospheres
H_o	arc chamber stagnation enthalpy, BTU/lb
T_o	arc chamber stagnation temperature, °R
P_{T_a}	impact pressure behind shock wave, mm Hg
P_e	nozzle exit wall static pressure, mm Hg
T_e	nozzle exit static temperature, °R
P_p	test section plenum chamber pressure, mm Hg
P_D	impact pressure at diffuser exit, mm Hg
P_{D_e}	diffuser exit wall static pressure, mm Hg
P_v	vacuum pump inlet pressure after model insertion, mm Hg
P_v^B	vacuum pump inlet pressure when P_e is 50 percent larger than its valve at fully expanded nozzle flow, i.e., flow collapsed, mm Hg
P_v^B/P_{T_a}	diffuser recovery pressure ratio
d_e	nozzle exit diameter, inches
d_D	diffuser throat diameter, inches
d_M	model base diameter, inches
A	flow core area, square inches
A_e	nozzle exit area, square inches
A_D	diffuser throat area, square inches
A_M	model base, area, square inches
A_M^B	largest model without blockage, square inches
A^*	nozzle throat area, square inches
L	diffuser throat length, inches
L/d_D	diffuser throat fineness ratio
W	plenum pumping rate in percent of tunnel mass flow

SYMBOLS (CONT'D)

A_M^B/A_e	ratio of largest model to nozzle exit area
M	Mach number
U	test section gas flow velocity, ft/sec
R_N	Reynolds number
ρ	static density, $\frac{\text{slugs}}{\text{ft}^3}$
$\dot{m}_T$	nozzle mass flow, lb/min
$\dot{m}_p$	plenum air pumping rate, lb/min

INTRODUCTION

A diffuser is required on a high Mach number wind tunnel to extend its operating range and run times. This is especially important for the Fifty-Megawatt Electrogasdynamic Facility now being constructed for the Research and Technology Division (RTD). In selecting a diffuser for this facility, consideration was given to its large size, continuous flow, high Mach number, low density, and high temperatures. All these factors influence the choice of a diffuser configuration, but probably the most critical one is high temperature. This is further complicated by a steep air temperature gradient near the flow boundary which is characteristic of the type of electric arc air heater used.

The Prototype Arc Facility utilizes a scaled-down version of the high voltage arc heater to be used on the Fifty-Megawatt Facility, thereby closely duplicating its temperature distribution. The selection of a diffuser for the Fifty-Megawatt Facility was based on the best compromise for pressure recovery and maximum model size.

DESCRIPTION

Test Facility

The investigations were performed in the One-Megawatt Prototype Electrogasdynamic Facility shown in Figures 1 and 2. This facility is a continuous-flow, free-jet tunnel that exhausts into a vacuum system. Stored 1200 psia air is passed through a silica gel drier and then to a continuous direct-current arc air heater capable of operating at 1000 KW. This heater is described in References 1 and 2. A 4.19-inch exit diameter conical nozzle with interchangeable throat sections can be used to obtain various test section flow conditions. The included expansion angle of the conical nozzle is 16°.

The test cabin is equipped with mounts for impact pressure survey probes and blockage models. The probe and models are stored outside the free-jet test flow during the tunnel starting process. The impact pressure probe was injected into the flow, using an electric actuator, at a location 0.25 inch downstream of the nozzle exit. The blockage models were injected by an air actuator to the tunnel centerline with injection times approximating one quarter of a second. The two locations were 0.50 inch downstream and 2.75 inches downstream of the nozzle exit.

The diffuser and model configurations are shown in Figure 3. The diffuser consisted of a convergent entrance scoop with a total included angle of 18 degrees, and a constant-area throat section. There was no divergent exit section.

The free-jet length (distance from nozzle exit to diffuser entrance) was held fixed at 7.5 inches.

A vacuum bypass valve allowing atmospheric air to bleed into the vacuum pumps was used to give variable back pressures (or, in effect, pump inlet pressures).

The test section plenum pumping line was connected at right angles to the flow and was 6 inches in diameter. Flow rates were measured using a calibrated orifice.

Manuscript released by author November 1963 for publication as an RTD Technical Documentary Report.

The entire test leg with the exception of the arc heater, sonic throat, and model struts was uncooled, thereby limiting the continuous run time of the facility to 15 minutes at the higher enthalpies.

The following calculated data are presented assuming equilibrium and frozen flow expansions (Reference 4). The basis for the calculation was the measured P_o, H_o, and $\dot{m}_T$.

P_o = 100 psia

T_o = 7380°R

H_o = 3000 BTU/lb

A_c/A^* = 280.

	Equilibrium	Frozen Flow	Measured
A/A^*	190	162	156
M	5.8	7.6	---
P_e, mm Hg	1.19	0.74	0.60-0.90
T_e, °R	1700	600	---
P_{T_2}, mm Hg	48.6	49.0	42
U, ft/sec	11,250	10,245	Centerline 10,000-10,300
R_N/ft	1.6×10^4	3.2×10^4	---
ρ, $\frac{\text{lb sec}^2}{\text{ft}^4}$	1.25×10^{-6}	1.40×10^{-6}	Centerline $1.235\text{-}1.29 \times 10^{-6}$

Facility Instrumentation

The arc heater voltage was measured using a calibrated voltmeter. The arc current was measured using a meter and shunt. Iron-constantan thermocouples were located in all the arc heater water inlet and outlet lines. The temperature rise in the coolant was recorded and used together with the water flow rate and tunnel mass flow to determine the stagnation enthalpy. A sonic orifice was located in the plenum pumping line and calibrated for various flow rates. The downstream side of the orifice was connected to a vacuum of 0.02 mm Hg, and the pressure ratio across the orifice was monitored to insure that sonic flow existed.

Pressure Instrumentation

Various pressure sensing instruments were used such that the full ranges of pressures could be measured. The arc chamber pressure was monitored by a bourdon-tube type pressure gage. All test section impact pressures were measured using a silicon oil U-Tube micromanometer referenced to a vacuum of less than 0.050 mm Hg absolute.

The test section plenum chamber pressure was determined by a CEC Magnavac thermal conductivity gage, and the nozzle exit pressure by a CEC Pirani gage. Pirani gages were also used to determine the flow through the plenum pumping line. All other pressures were measured with Wallace-Tiernan gages. All instruments were check-calibrated before and after the tests.

The local velocity and density were measured utilizing a local induction mass-flow probe and an impact pressure probe. These probes were designed and constructed by laboratory personnel.

Blockage Models

Thirteen 60-degree blunted cone models (Figure 4) were used to define the operating limits of the diffuser with a representative model in the hot air flow. The models varied in base diameter from 0.5 inch to 2.375 inches, but were geometrically similar. All cones were made of solid carbon, and were uncooled during the test. They were heated to incandescence while in the hot flow, but were allowed to cool before reinsertion. The model blockage ratio is defined as the ratio of the model base area to the geometrical nozzle exit area.

The models were mounted on a cooled movable support (Figure 5) to facilitate insertion into the flow as rapidly as possible. A 0.312-inch-diameter water-cooled sting and strut were used to support the models. A 30-degree included-angle cooled leading edge was placed on the strut in order to relieve the strut blockage.

Test Procedures

The tunnel was brought to desired operating condition with the test section empty. A complete nozzle impact pressure survey was made for each nozzle-diffuser configuration. A typical survey is presented in Figure 6.

A typical diffuser blockage test proceeded as follows. Flow was established and stabilized at the desired operating condition. The vacuum pump inlet pressure was raised by bleeding in air downstream of the diffuser, and taking data until the nozzle exit pressure increased to one and one-half times the value at fully expanded nozzle flow, indicating possible flow separation. This point was noted as P_v^B. Data were taken prior to inserting the model and after the model was on the tunnel centerline. The model was removed from the flow between data points. The pump inlet pressure was recorded prior to inserting the model. When flow collapsed on a model due to blockage, the model was removed from the flow, plenum pumping turned on full, and the model reinserted into the flow for data collection. The plenum pumping rate was then reduced until the flow again collapsed on the model. This was called the minimum plenum pumping rate required for each tunnel-model configuration.

All data were hand-recorded and hand-reduced.

Data Accuracy

A summary of possible errors is given below:

P_o	±5 psia
H_o	±200 BTU/lb

P_{T_a}	±1 mm Hg
P_e	±0.010 mm Hg
P_p	±0.050 mm Hg
P_D	±0.150 mm Hg
P_{D_e}	±0.080 mm Hg
P_v	±0.050 mm Hg
P_v^B	±1 mm Hg
$\dot{m}_p$	±0.003 lb/min
$\dot{m}_T$	±0.03 lb/min

The sealing of the test chamber was accomplished with "O" rings, gaskets, and high-vacuum grease. The leak rate of the test leg was kept to less than 1% of tunnel mass flow throughout the test.

RESULTS

Two diffuser configurations not shown in this report were also run. The first, with $A_D/A_e = 0.75$, would not allow tunnel flow to start with an empty test section. The second, with $A_D/A_e = 0.942$ and $L/d_D = 4$, gave a tunnel-empty (no model) recovery of only 9.5 percent. These diffusers, similar to the ones in this report, but shorter and with smaller throat diameters, were considered unsuitable and were not utilized thereafter.

A typical test section impact pressure survey is presented in Figure 6, and test section flow pictures in Figures 7 and 8. Basic performance curves for all diffusers tested are presented in Figures 9 through 22. The best tunnel-empty pressure recovery (Figure 23) occurred with the 94 percent diffuser, and was independent of length in the range tested. The flow in the 119 percent diffuser throat remained supersonic with L/d_D of 9 and was decelerated to subsonic with lengths longer than 12 diameters. The effects on blockage model sizes of changing the diffuser throat area are shown in Figure 24. Good test flow could be maintained with a 24.2 percent model when the long ($L/d_D = 22$) diffusers with large throat areas (119%-145%) were used. The addition of plenum pumping resulted in little increase in allowable model size at $A_D/A_e = 119$ percent, but gave significant increases with the other two diffusers. Only small models could be inserted in the flow with the 94 percent diffuser regardless of its throat length. Very little effect of diffuser throat length on model size is noted with a 94 percent diffuser (Figure 25). This is probably due to its exit flow always being subsonic regardless of length. Significant increases in maximum model sizes occurred as the diffuser throat length was increased while holding the diffuser throat area constant at 119 percent. The diffuser exit flow changed from supersonic to subsonic as the throat length was increased. This transition occurred at about $L/d_D = 12$. Increasing the diffuser throat area to 145 percent allowed 24.2 percent models

to be inserted in the flow at all diffuser throat lengths without changing the nozzle exit pressure and plenum pressures. Diffuser exit pressure ratios indicate the flow there to be supersonic at all conditions, therefore the maximum allowable model size remained essentially constant. Doubling the stagnation enthalpy had essentially no effect on diffuser pressure recovery (Figure 26).

The effect of increasing the model size on diffuser pressure recovery can be seen in Figure 27. As would be expected, the pressure recovery decreases as the model size increases. The 119 percent diffuser pressure recovery was least affected by the increasing model size when the throat length was 22 diameters. The diffuser recovery pressure ratio was maintained greater than 40 percent with model sizes 20 percent or less. The results of plenum pumping are also shown in Figure 27.

Shortening the model support sting resulted in smaller allowable model sizes and less diffuser pressure recovery. These data are not summarized, but are included in the basic performance curves.

CONCLUSIONS

Tests on model blockage and diffuser pressure recovery were made in air electric arc wind tunnel delivering approximately 125 KW to the 4-inch-diameter free-jet test airflow. The Mach number was 7.6 and the total enthalpy 3000 BTU/lb.

Considering both the pressure recovery and the maximum allowable model size, the best diffuser tested had a cross-sectional area 19 percent larger than the nozzle exit area and a diffuser length-to-diameter ratio of 15. The tunnel-empty diffuser recovery pressure was 43 percent of the test section pitot pressure. It decreased to 33 percent upon inserting into the test flow a 60-degree blunted cone model having a frontal area of 20 percent of the nozzle exit area.

Vacuum pumping from the test section plenum did not significantly increase the maximum model size. Increasing the flow enthalpy from 3000 to 6000 BTU/lb had no effect on the tunnel-empty pressure recovery.

REFERENCES

1. R. C. Eschenbach and G. M. Skinner, Study of Arc Heaters for A Hypersonic Wind Tunnel, WADD-TR-60-354, May 1960.

2. R. C. Eschenbach and G. M. Skinner, Development of Stable, High Power, High Pressure Arc Air Heaters for A Hypersonic Wind Tunnel, WADD-TR-61-100, July 1961.

3. S. L. Petrie and N. E. Scaggs, Experimental Studies of Hypersonic Wind Tunnel Diffusers, Ohio State University TN 561-1, October 1961.

4. K. Pearce, S. Samet, and R. J. Whalen, Similarity Studies for Dissociating Gases in Hypersonic, Low Density Flow, WADD-TR-60-341, September 1960.

APPENDIX

TEST SETUP AND DATA

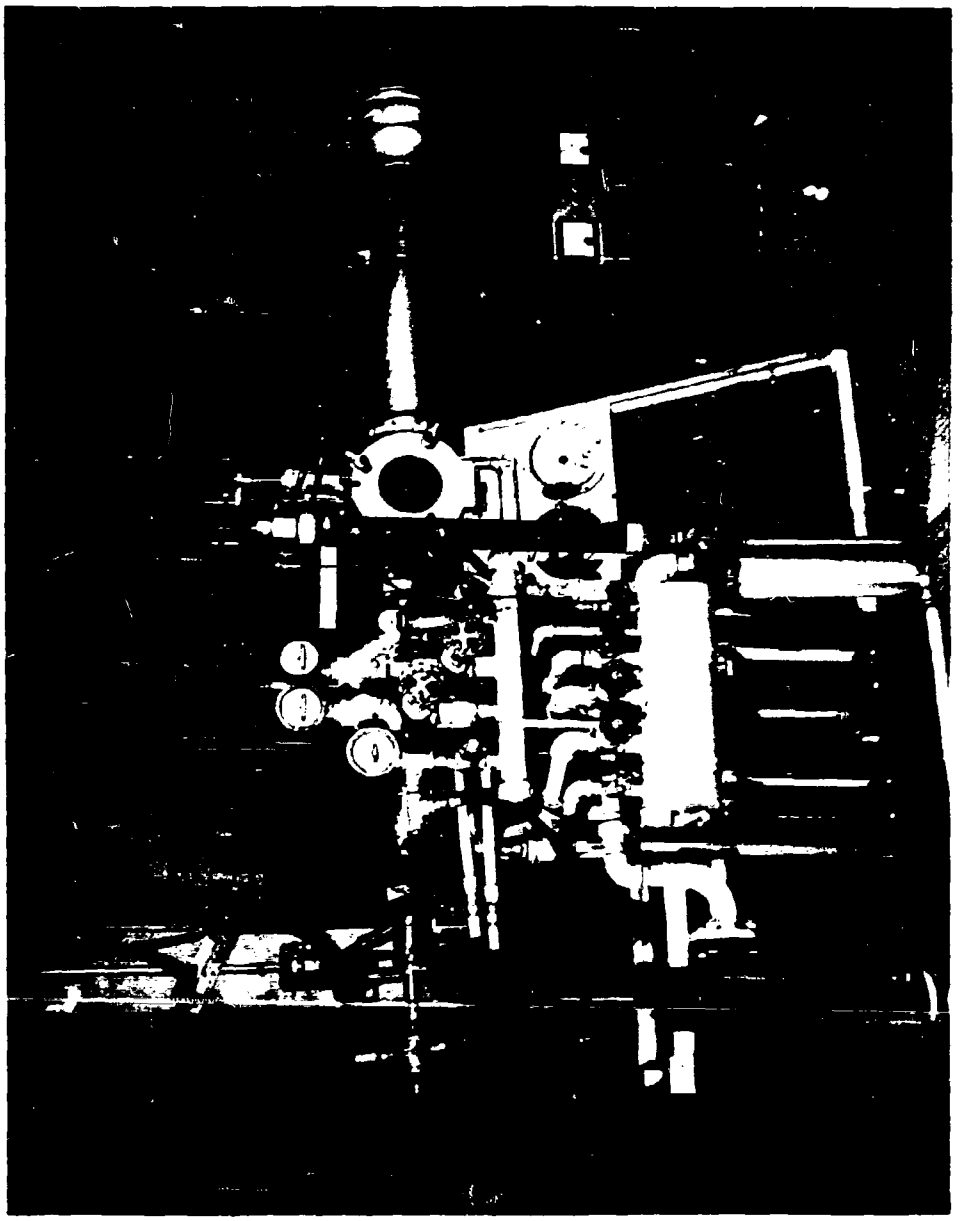

Figure 1. Prototype Arc Facility

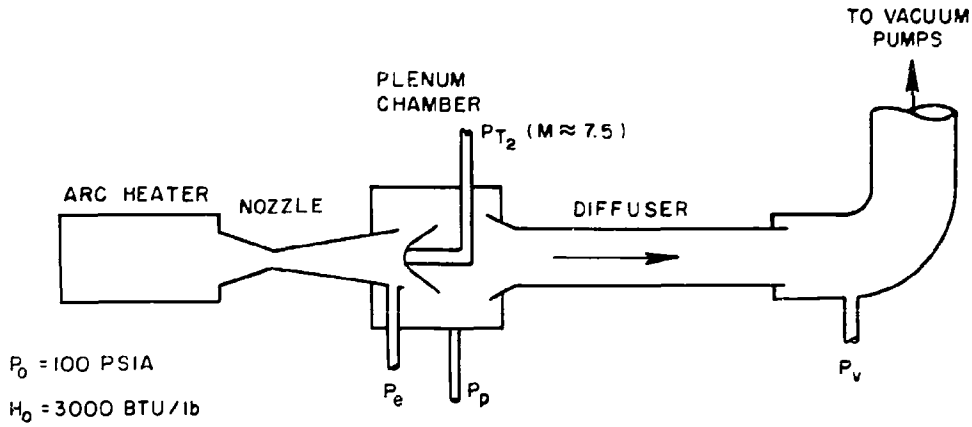

Figure 2. Tunnel Schematic

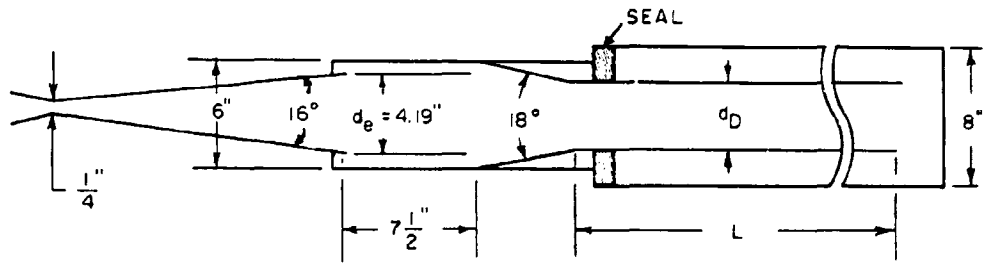

DIFFUSER

DIFFUSER	$\frac{L}{d_D}$	$\frac{d_D}{d_e}$	$\frac{A_D}{A_e}$
I	24.2	0.970	0.942
II	21.6	1.090	1.190
III	20.0	1.20	1.450
IV	9.0	0.970	0.942
V	9.0	1.090	1.190
VI	9.0	1.20	1.450
VII	15.0	1.090	1.190
VIII	12.0	1.090	1.190

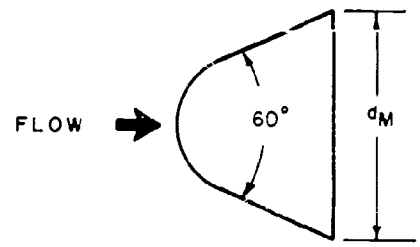

BLOCKAGE MODELS

Figure 3. Diffuser Configurations

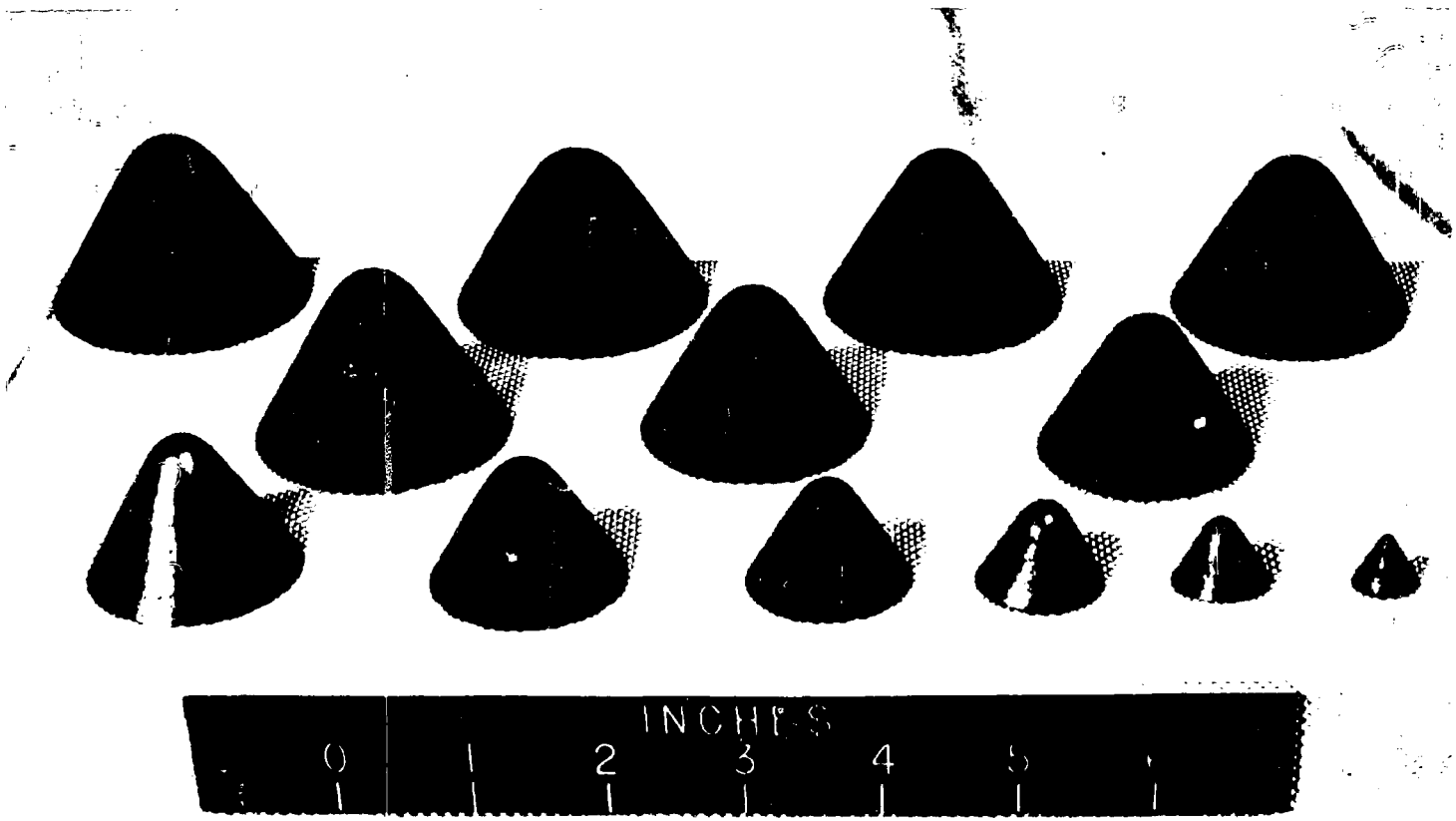

Figure 4. Carbon Blockage Models

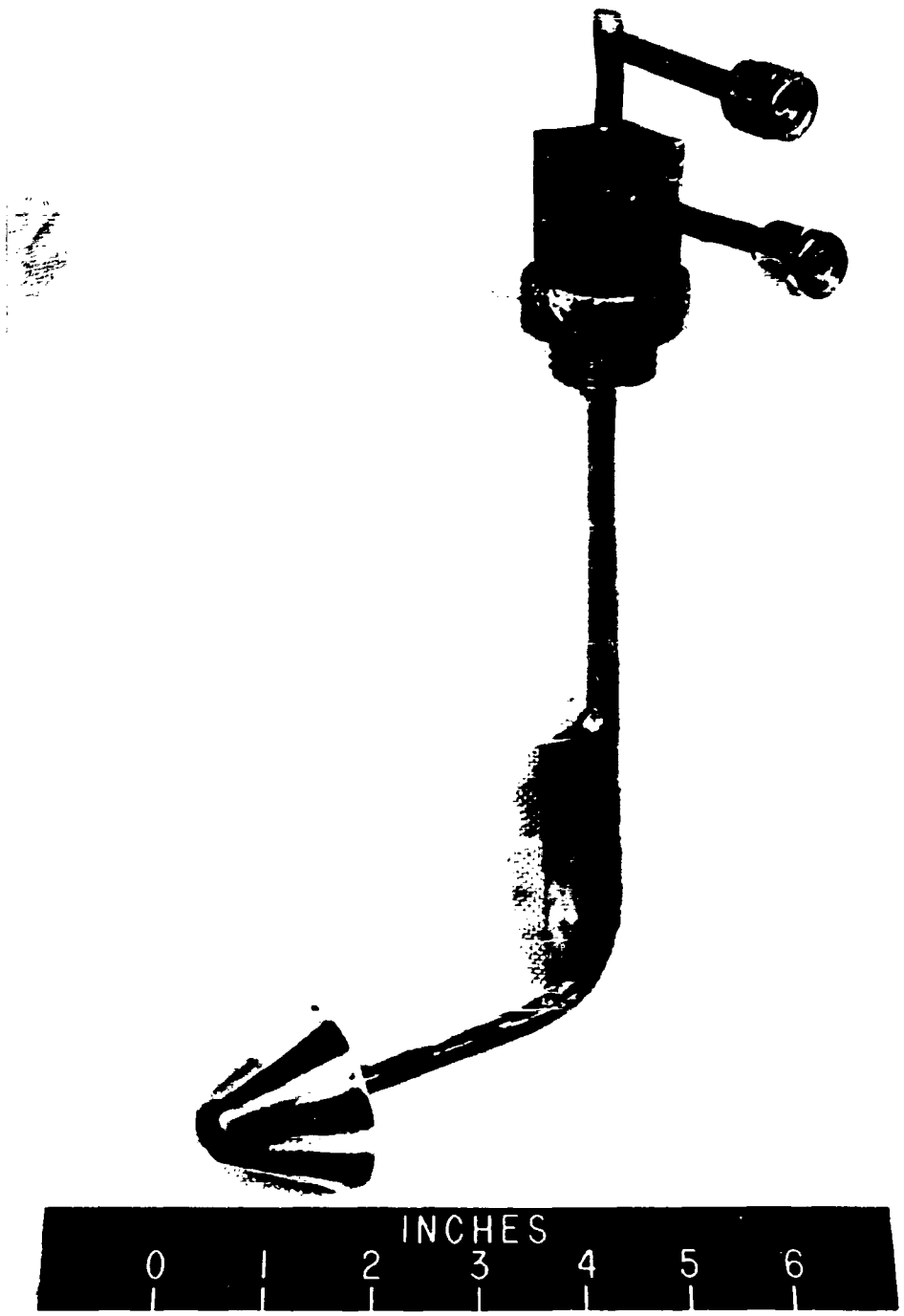

Figure 5. Blockage Model Strut

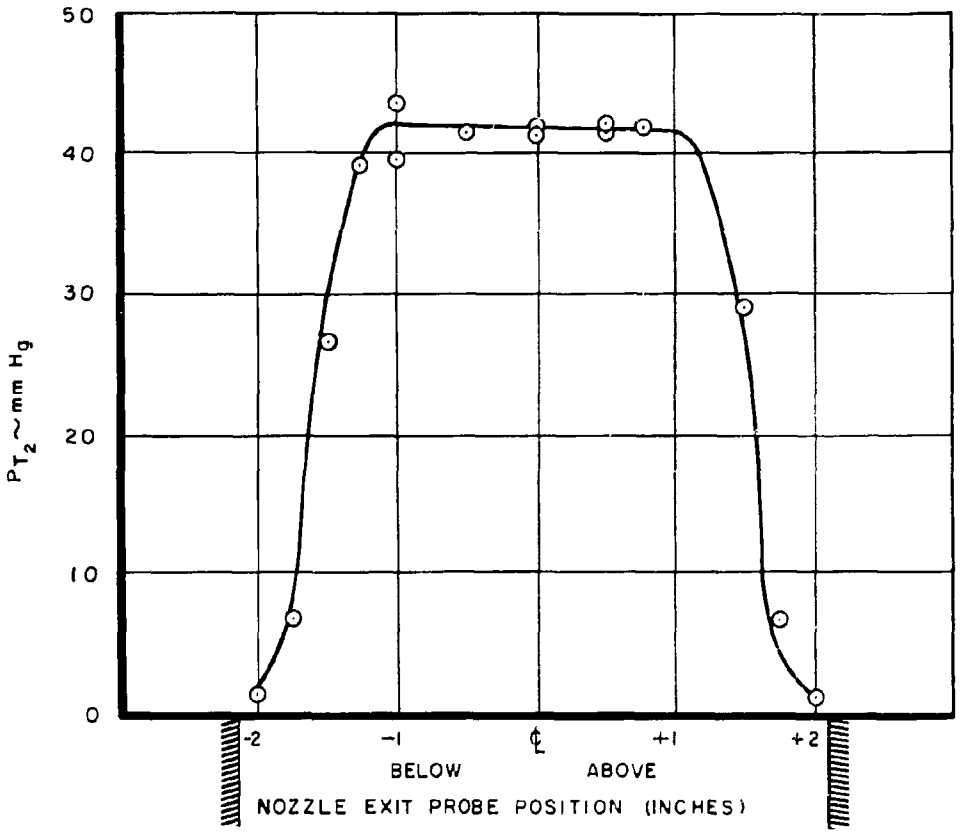

Figure 6. Typical Impact Pressure Survey

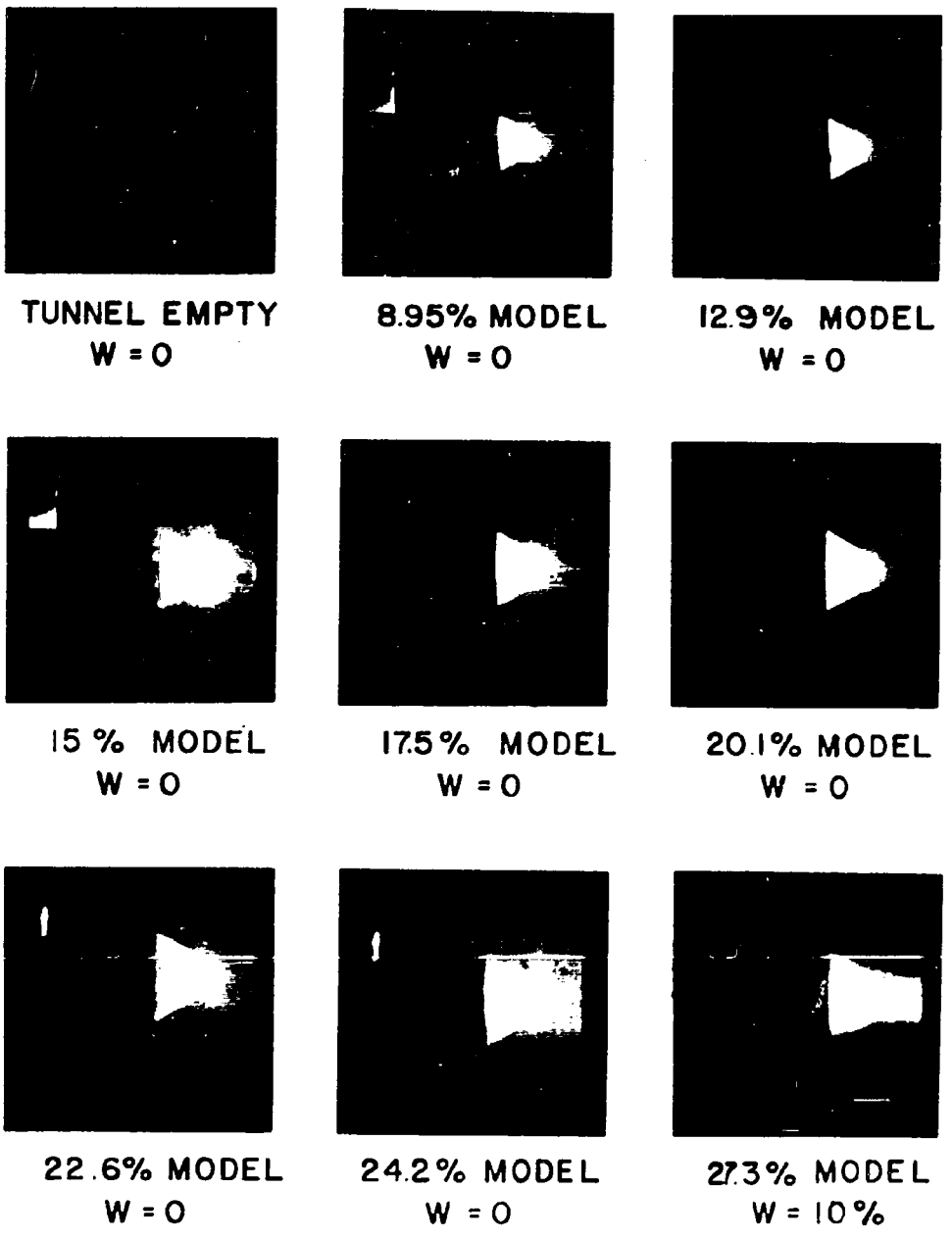

Figure 7. Flow Pictures Using Diffuser II With Long Sting

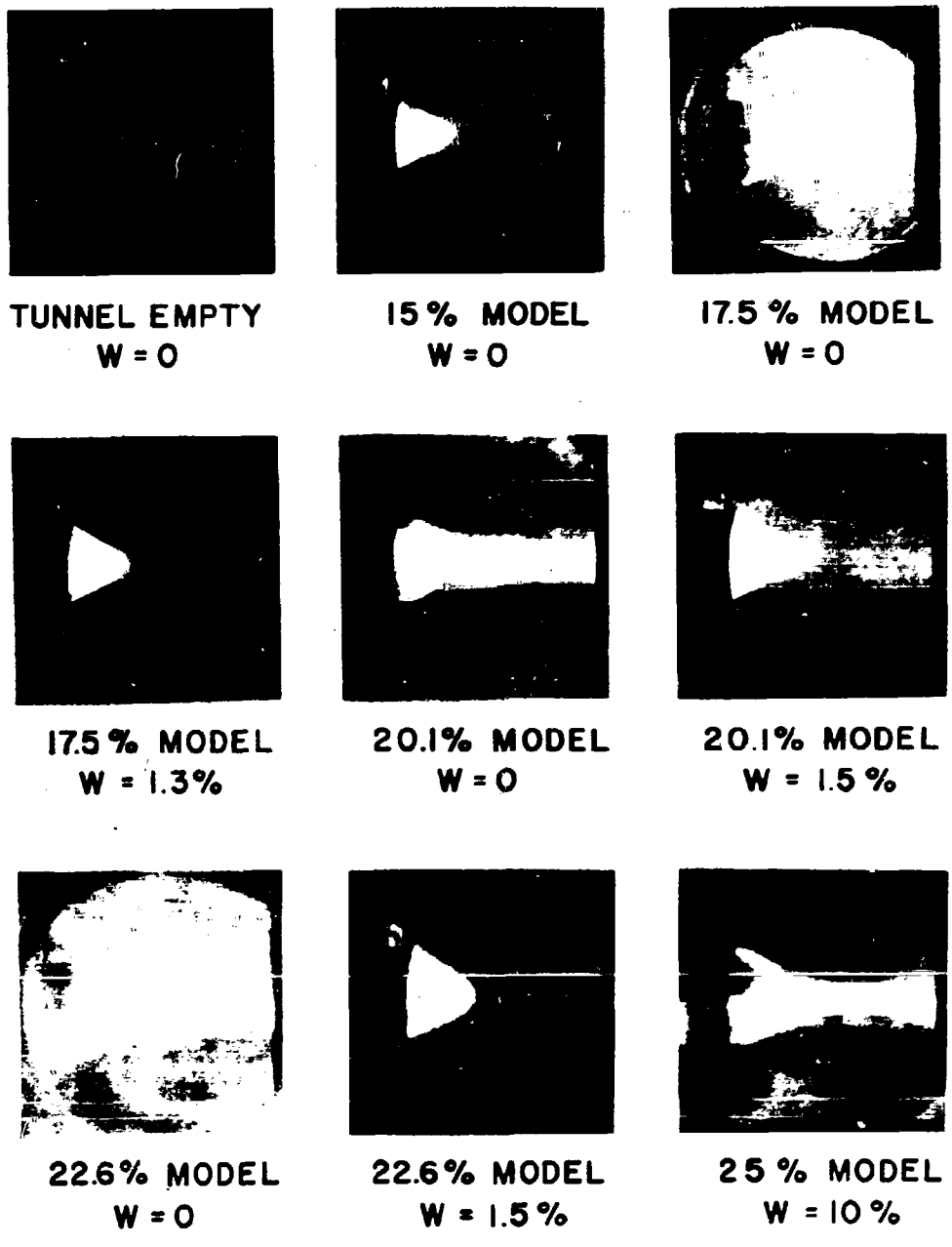

Figure 8. Flow Pictures Using Diffuser II With Short Sting

TEST CONDITIONS			
P_p	P_e	Model Size	Minimum Plenum Pumping Required
●	⊙	None	None
▲	△	12.9 %	None
▼	▽	15.0 %	W = 2.8 %
■	⊡	17.5 %	W = 4.5 %

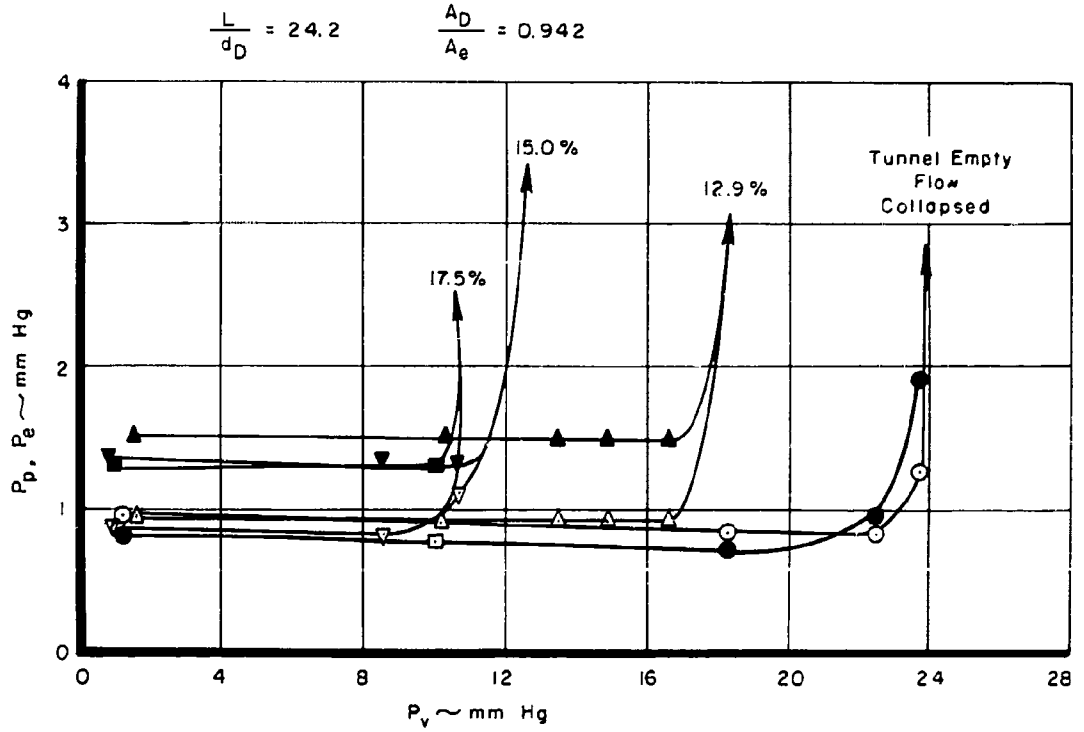

Figure 9. Vacuum Pump Inlet Pressure Effects - Diffuser I, Long Sting

TEST CONDITIONS			
P_{D_e}	P_D	Model Size	Minimum Plenum Pumping Required
●	⊙	None	None
▲	△	12.9 %	None
▼	▽	15.0 %	W = 2.8 %
■	⊡	17.5 %	W = 4.5 %

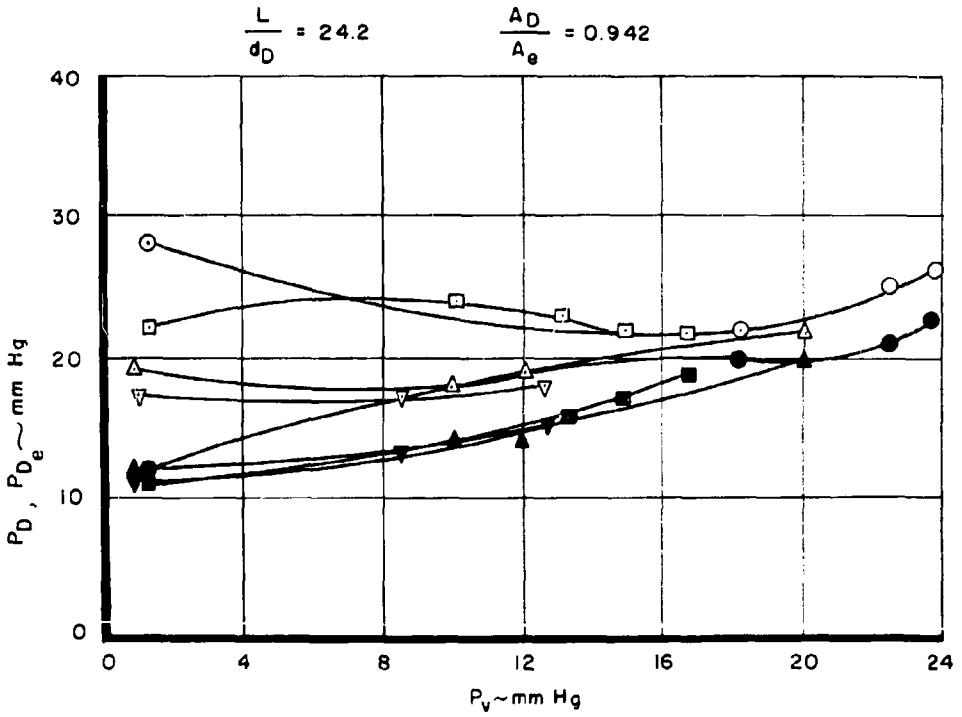

Figure 9. (Cont'd)

TEST CONDITIONS			
P_p	P_e	Model Size	Minimum Plenum Pumping Required
●	⊙	None	None
▲	△	12.9 %	None
▼	▽	15.0 %	W = 1.1 %
■	⊡	17.5 %	W = 4.5 %

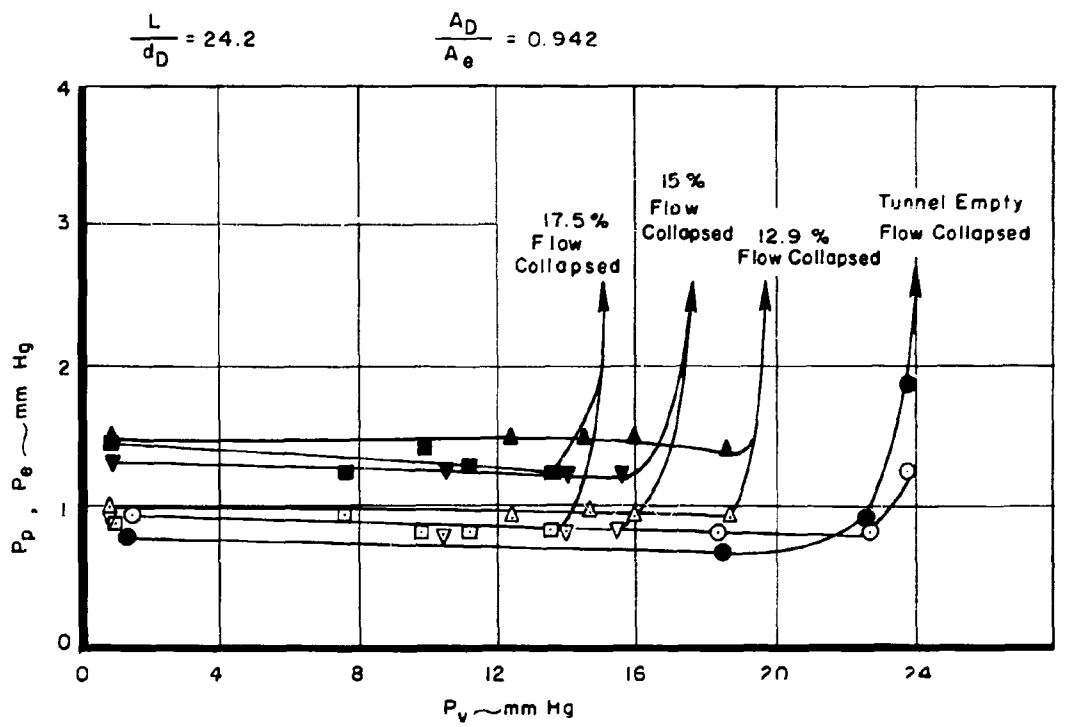

Figure 10. Vacuum Pump Inlet Pressure Effects - Diffuser I, Short Sting

TEST CONDITIONS			
P_{D_e}	P_D	Model Size	Minimum Plenum Pumping Required
●	⊙	None	None
▲	△	12.9 %	None
▼	▽	15.0 %	W = 1.1 %
■	⊡	17.5 %	W = 4.5 %

$\frac{L}{d_D} = 24.2$ $\frac{A_D}{A_e} = 0.942$

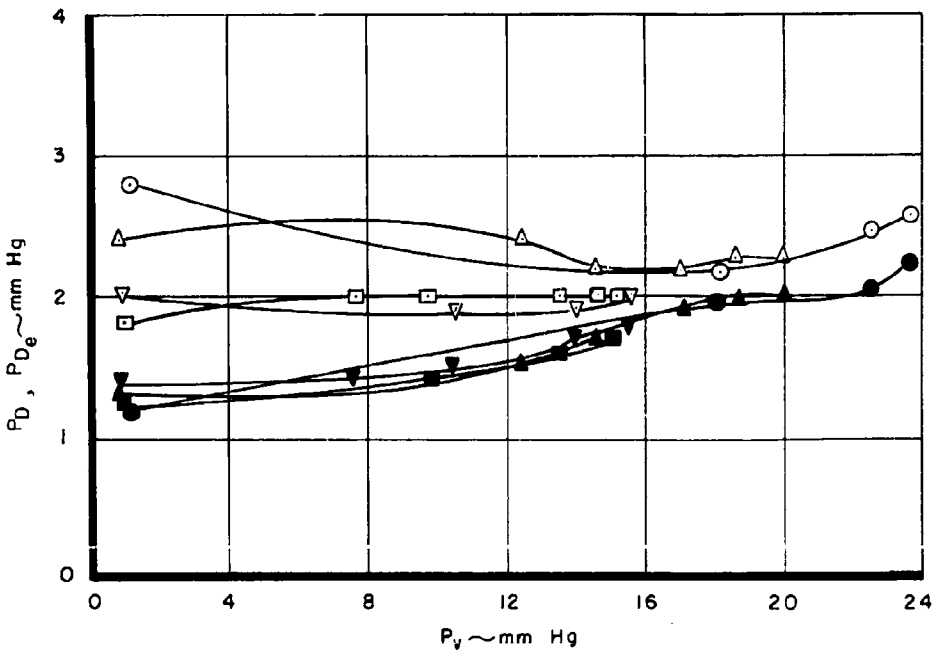

Figure 10. (Cont'd)

TEST CONDITIONS			
P_p	P_e	Model Size	Minimum Plenum Pumping Required
●	⊙	None	None
♦	◊	8.9%	None
■	□	17.5%	None
•	∘	20.1%	None
⬬	⬭	22.6%	None
▲	△	24.2%	None

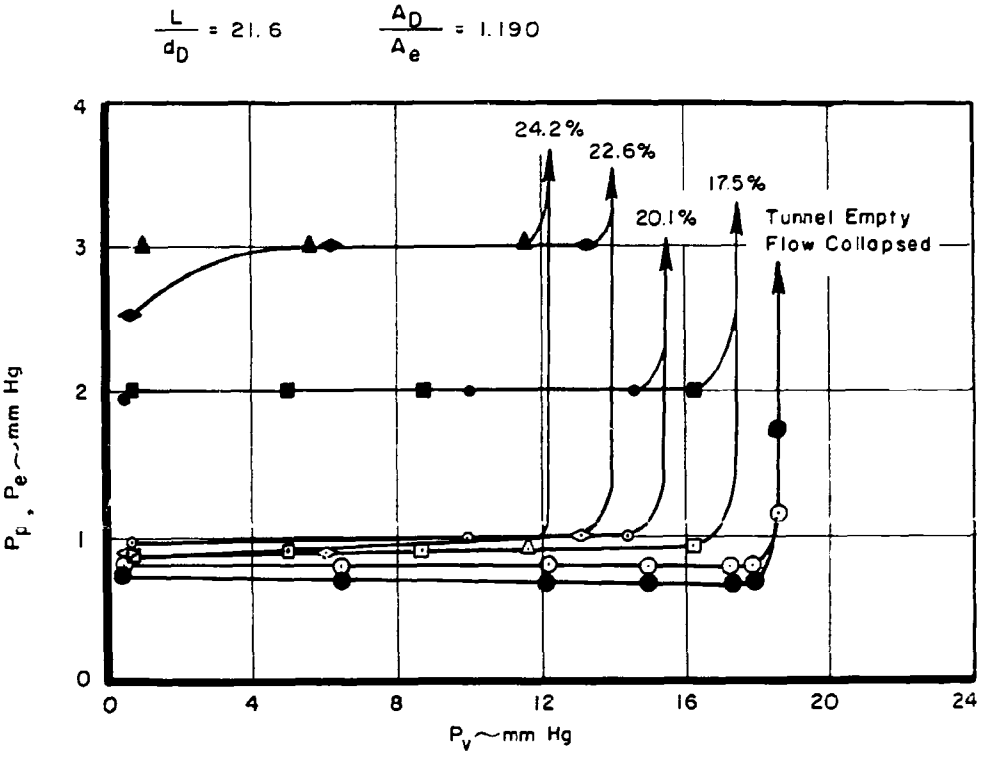

Figure 11. Vacuum Pump Inlet Pressure Effects - Diffuser II, Long Sting

TEST CONDITIONS			
P_{D_e}	P_D	Model Size	Minimum Plenum Pumping Required
●	⊙	None	None
♦	◊	8.9 %	None
▼	▽	12.9 %	None
■	⊡	17.5 %	None
•	⊙	20.1 %	None
◆	◇	22.6 %	None
▲	△	24.2 %	None

$\frac{L}{d_D} = 21.6$ $\frac{A_D}{A_e} = 1.190$

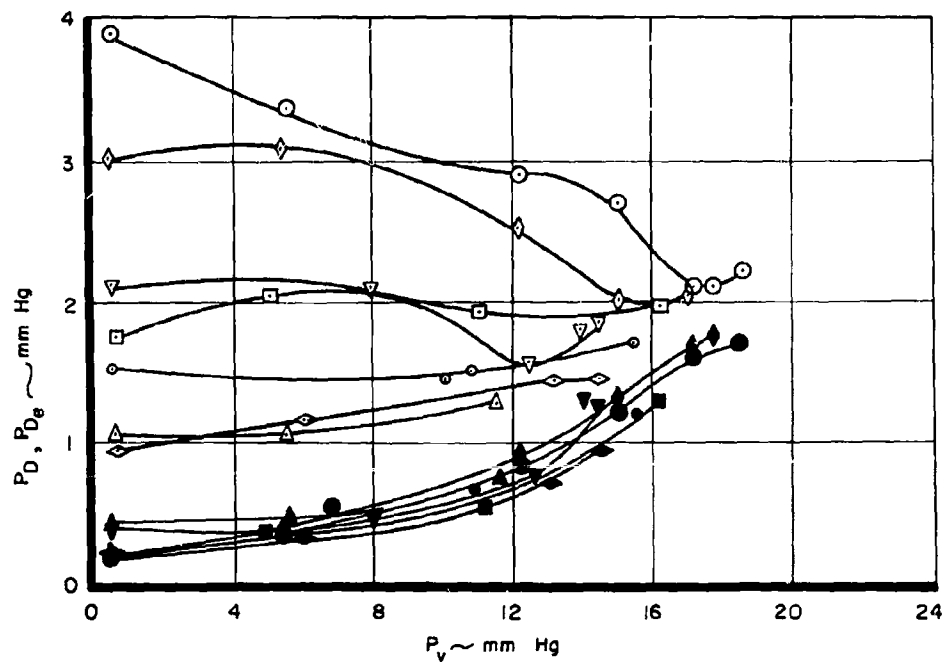

Figure 11. (Cont' d)

TEST CONDITIONS			
P_p	P_e	Model Size	Minimum Plenum Pumping Required
●	⊙	None	None
■	⊡	15.0%	None
▼	▽	17.5%	W = 1.3%
♦	◊	20.1%	W = 1.5%
▲	△	22.6%	W = 1.5%

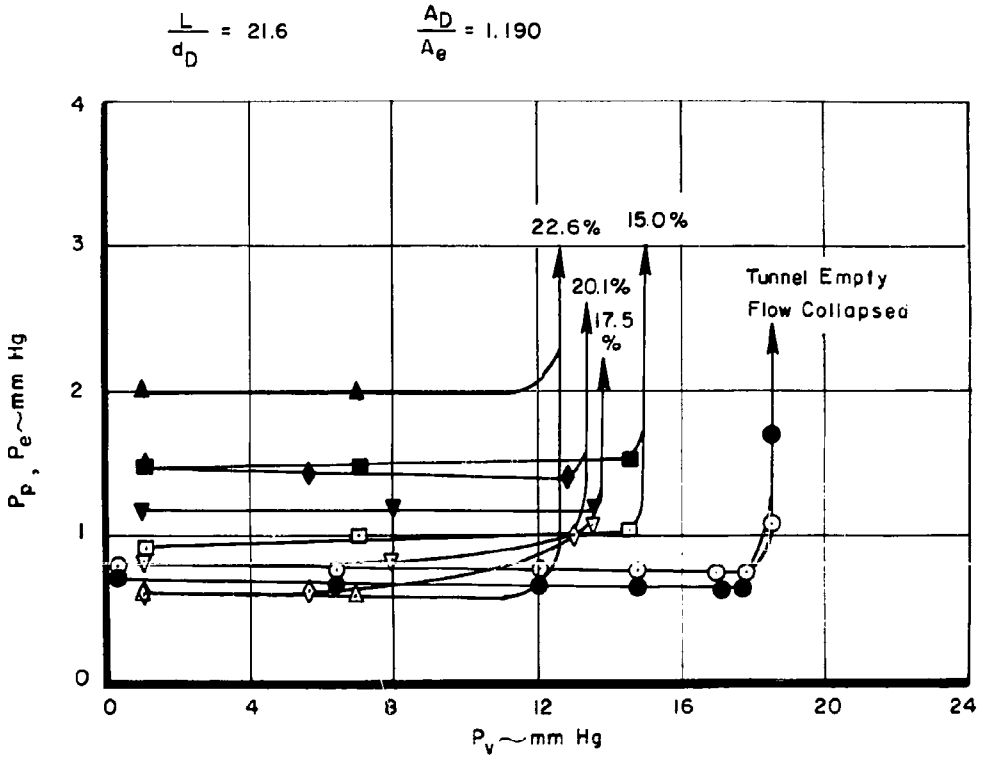

Figure 12. Vacuum Pump Inlet Pressure Effects - Diffuser II, Short Sting

TEST CONDITIONS			
P_D	P_{D_e}	Model Size	Minimum Plenum Pumping Required
●	⊙	None	None
■	⊡	15.0 %	None
▼	▽	17.5 %	W = 1.0 %
♦	◊	20.1 %	W = 1.0 %
▲	△	22.6 %	W = 1.0 %

$\frac{L}{d_D} = 21.6$ $\frac{A_D}{A_e} = 1.190$

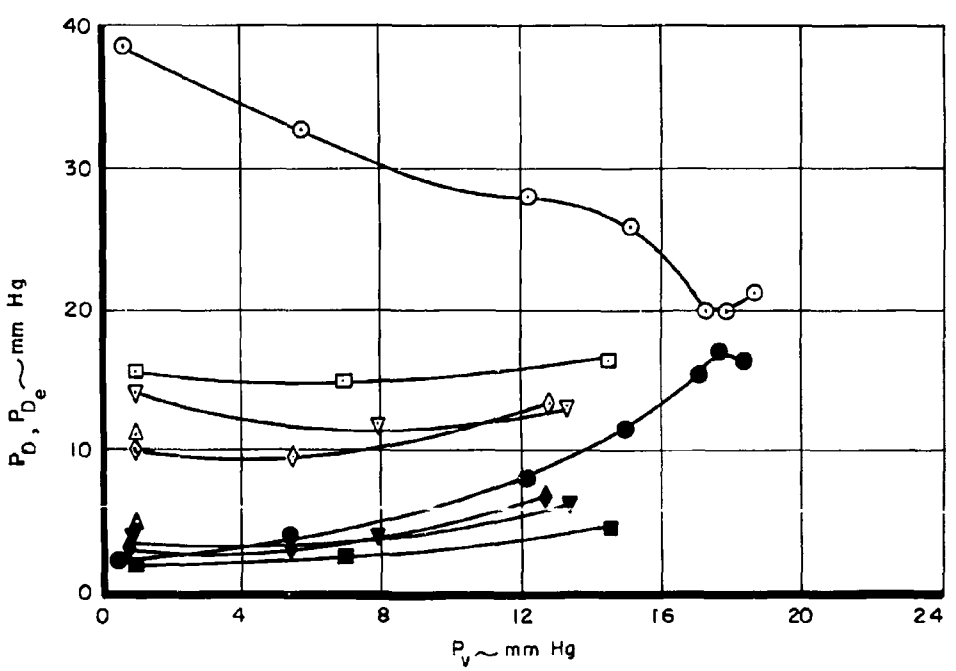

Figure 12. (Cont'd)

TEST CONDITIONS			
P_p	P_e	Model Size	Minimum Plenum Pumping Required
●	⊙	None	None
▲	△	12.9%	None
♦	◇	22.6 %	None
▼	▽	24.2 %	None
•	⊙	27.3 %	W = 4.7%

$\frac{L}{d_D} = 20.0$ $\frac{A_D}{A_e} = 1.450$

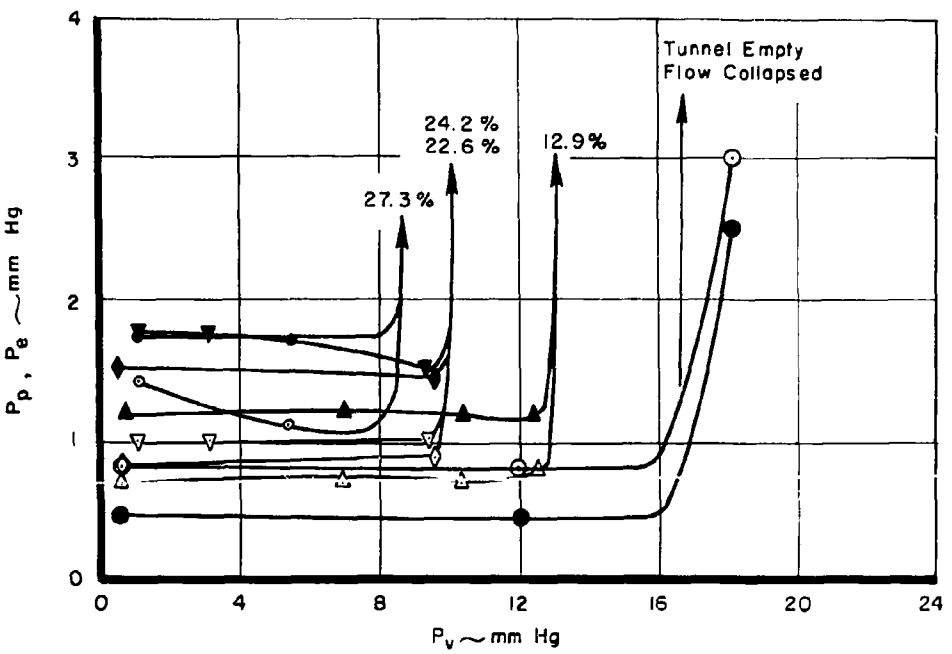

Figure 13. Vacuum Pump Inlet Pressure Effects - Diffuser III, Long Sting

TEST CONDITIONS			
P_{D_e}	P_D	Model Size	Minimum Plenum Pumping Required
●	⊙	None	None
▲	△	12.9%	None
♦	◊	22.6%	None
▼	▽	24.2%	None
•	⊙	27.3%	W= 4.7%

$\frac{L}{d_D} = 20.0$ $\frac{A_D}{A_e} = 1.450$

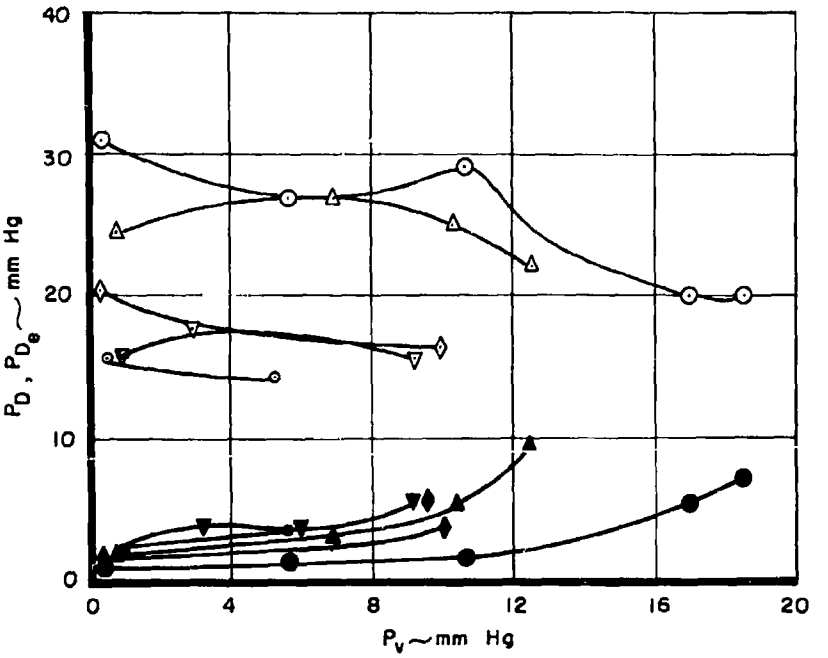

Figure 13. (Cont' d)

TEST CONDITIONS			
P_p	P_e	Model Size	Minimum Plenum Pumping Required
●	⊙	None	None
◆	◊	15.0 %	None
▼	▽	17.5 %	None
■	□	22.6 %	W = 1.0 %
●	⊙	24.2 %	W = 1.7 %
◆	◇	25.7 %	W = 0.8 %
▲	△	27.3 %	W = 4.3 %

$\frac{L}{d_D} = 20.0$ $\frac{A_D}{A_e} = 1.450$

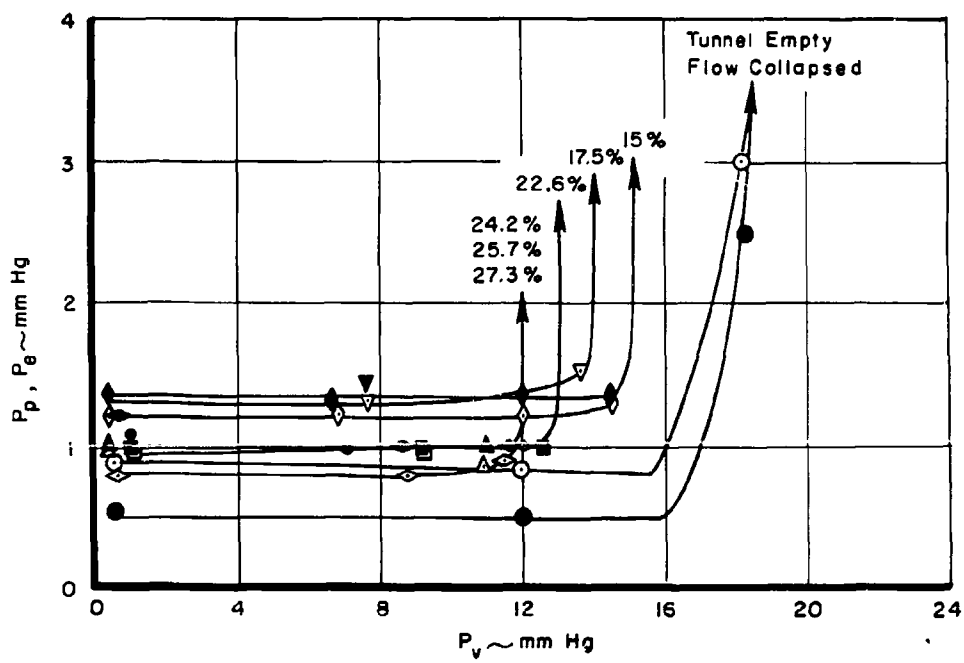

Figure 14. Vacuum Pump Inlet Pressure Effects - Diffuser III, Short Sting

TEST CONDITIONS			
P_{D_e}	P_{D_e}	Model Size	Minimum Plenum Pumping Required
●	⊙	None	None
♦	◊	15.0 %	None
▼	▽	17.5 %	None
■	⊡	22.6 %	W = 1.0%
●	⊙	24.2 %	W = 1.7%
◆	◇	25.7 %	W = 0.8 %
▲	△	27.3 %	W = 4.3 %

$\frac{L}{d_D} = 20.0$ $\frac{A_D}{A_e} = 1.450$

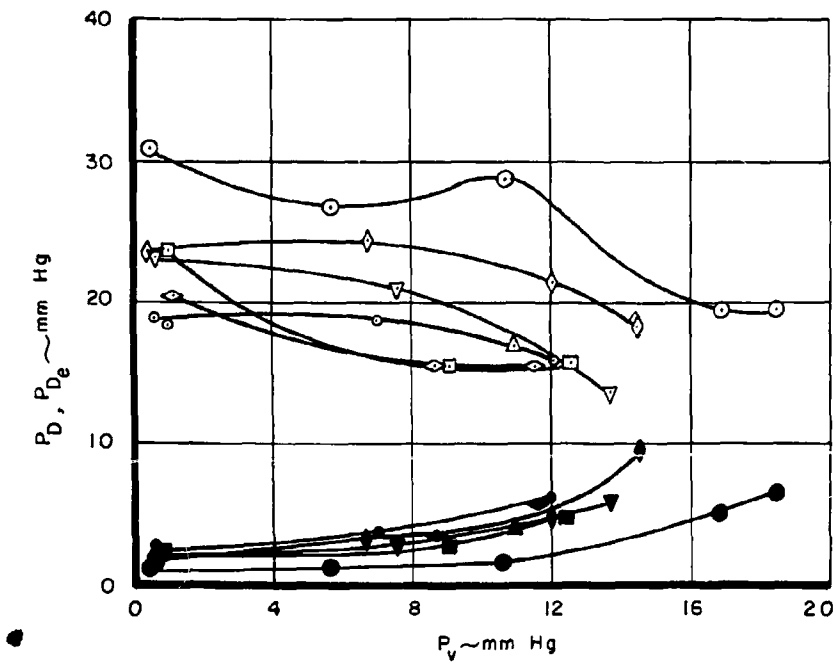

Figure 14. (Cont' d)

TEST CONDITIONS			
P_p	P_e	Model Size	Minimum Plenum Pumping Required
●	○	None	None
▲	△	5.7 %	None
♦	◇	8.95 %	None
■	□	15.0 %	None
▼	▽	17.5 %	W = 8.0 %

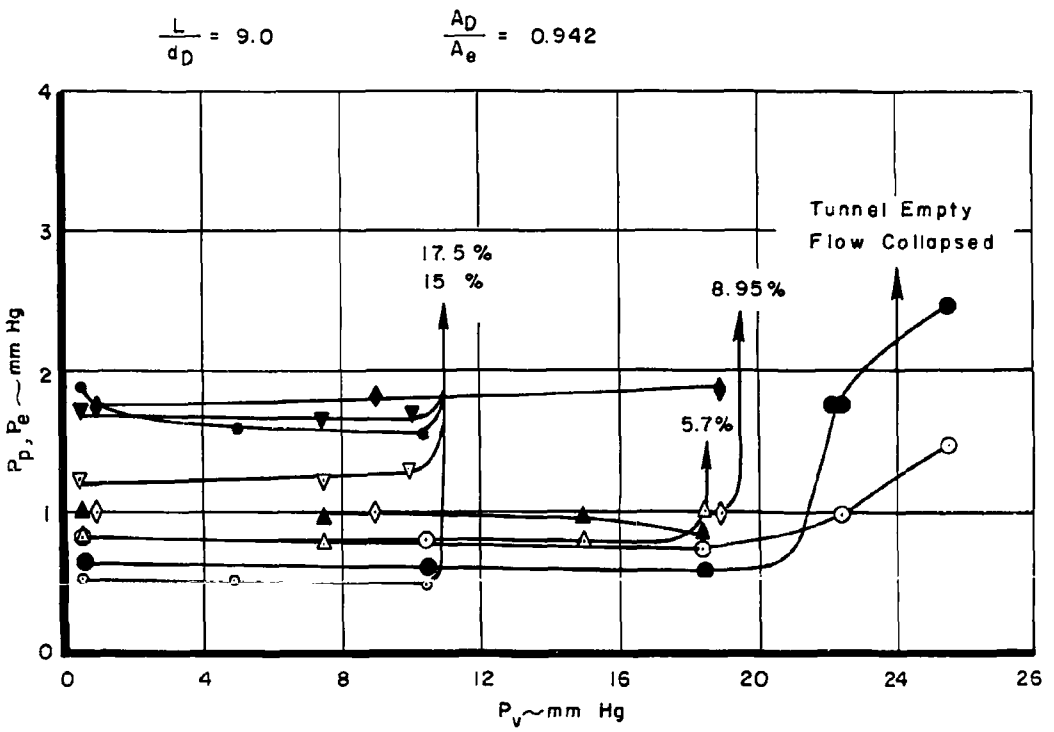

Figure 15. Vacuum Pump Inlet Pressure Effects - Diffuser IV, Long Sting

TEST CONDITIONS			
P_{D_e}	P_D	Model Size	Minimum Plenum Pumping Required
●	⊙	None	None
▲	△	5.7 %	None
◆	◇	8.9 %	None
•	⊙	15.0 %	None
▼	▽	17.5 %	None

$\frac{L}{d_D} = 9.0$ $\frac{A_D}{A_e} = 0.942$

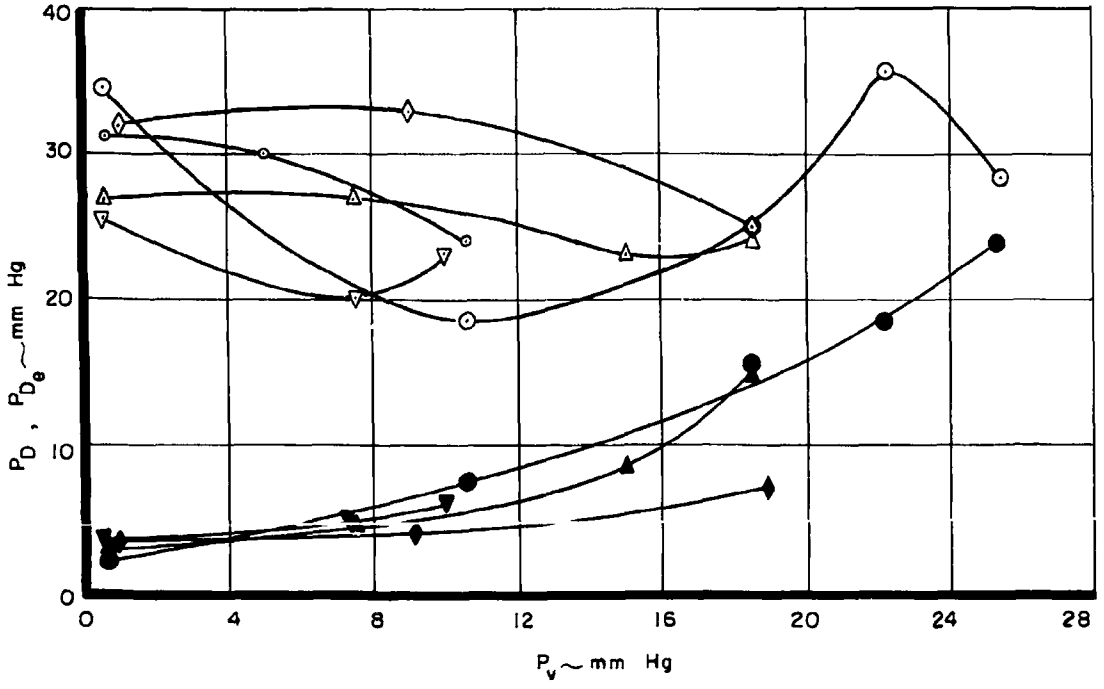

Figure 15. (Cont' d)

TEST CONDITIONS			
P_p	P_e	Model Size	Minimum Plenum Pumping Required
●	⊙	None	None
▲	△	8.9 %	None
♦	◇	12.9 %	None
•	⊙	15.0 %	W= 1.4 %
▼	▽	17.5 %	W= 8.5 %

$\frac{L}{d_D} = 9.0$ $\frac{A_D}{A_e} = 0.942$

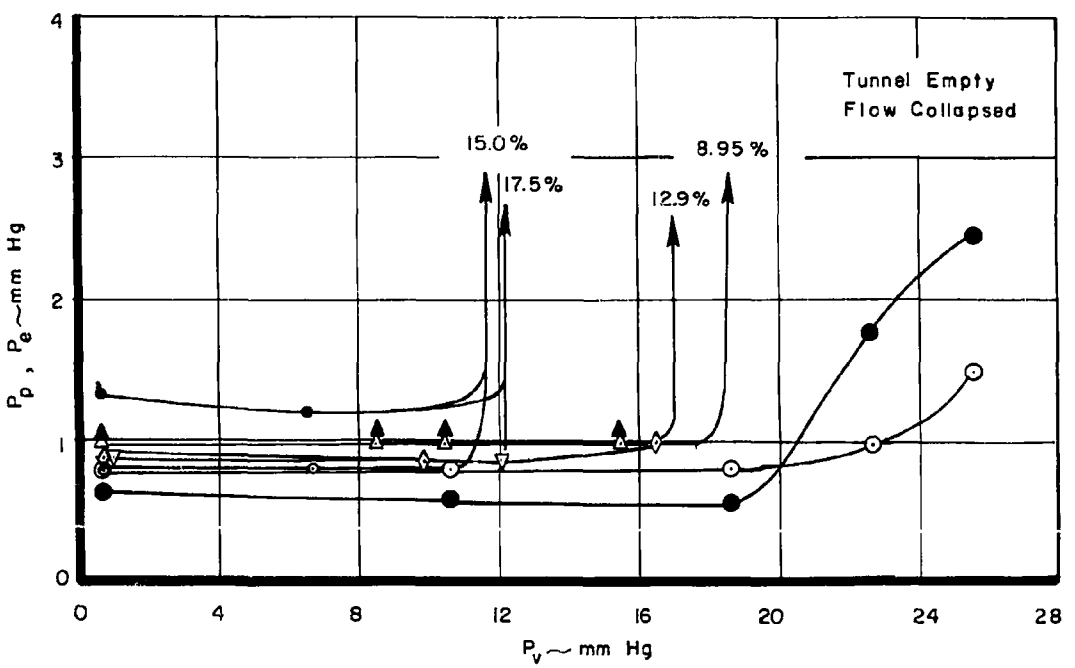

Figure 16. Vacuum Pump Inlet Pressure Effects - Diffuser IV, Short Sting

TEST CONDITIONS			
P_{D_e}	P_D	Model Size	Minimum Plenum Pumping Required
●	⊙	None	None
▲	△	8.9 %	None
♦	◊	12.9 %	None
●	⊙	15.0 %	W = 1.3 %
▼	▽	17.5 %	W = 8.7%

$\frac{L}{d_D} = 9.0$ $\frac{A_D}{A_e} = 0.942$

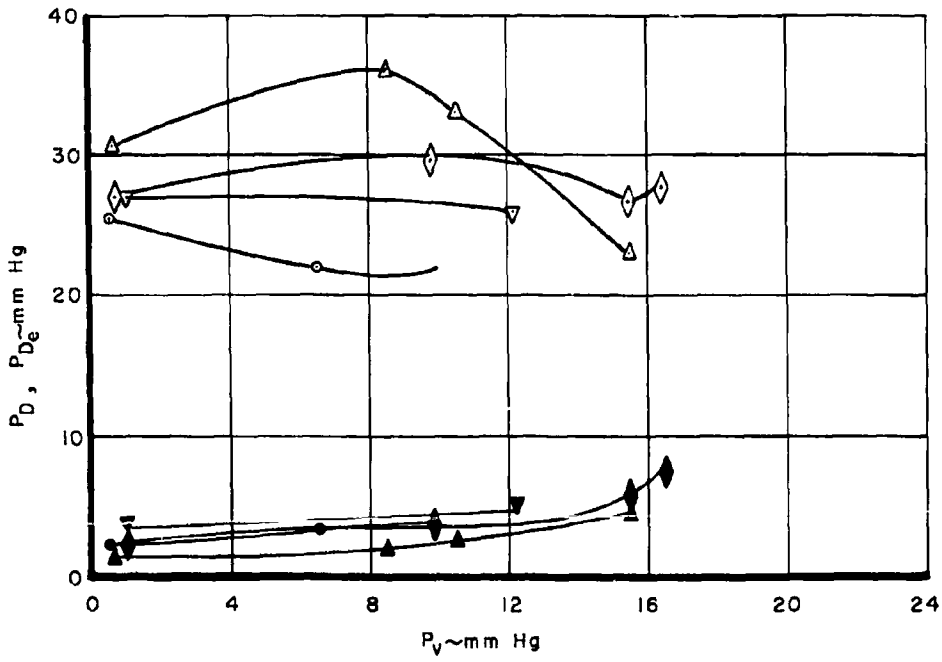

Figure 16. (Cont' d)

TEST CONDITIONS			
P_p	P_e	Model Size	Minimum Plenum Pumping Required
●	⊙	None	None
▲	△	8.95 %	None
♦	◇	17.5 %	None
•	⊙	20.1 %	W = 1.9 %

$\frac{L}{d_D} = 9.0$ $\frac{A_D}{A_e} = 1.190$

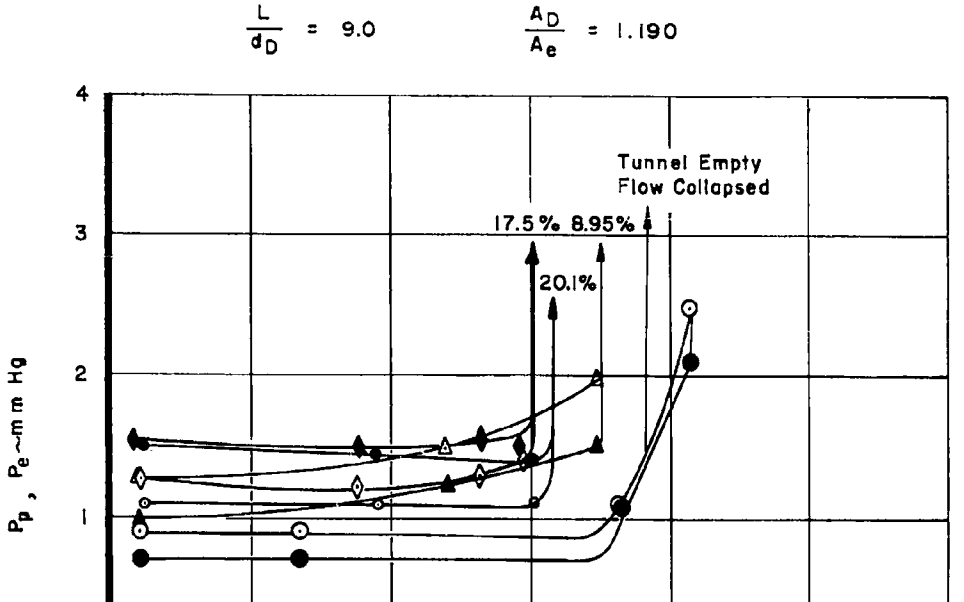

Figure 17. Vacuum Pump Inlet Pressure Effects - Diffuser V, Long Sting

TEST CONDITIONS			
P_p	P_e	Model Size	Minimum Plenum Pumping Required
●	⊙	None	None
▲	△	8.9 %	None
♦	◇	17.5 %	None
•	⊙	20.1 %	W = 1.9 %

$\frac{L}{d_D} = 9.0$ $\frac{A_D}{A_e} = 1.190$

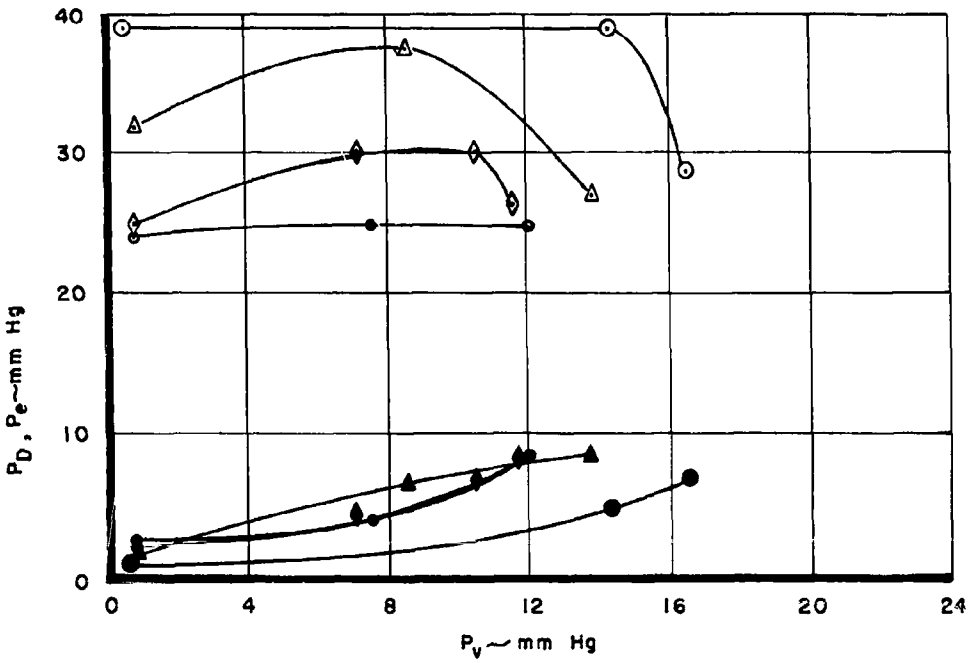

Figure 17. (Cont' d)

TEST CONDITIONS			
P_p	P_e	Model Size	Minimum Plenum Pumping Required
●	⊙	None	None
▲	△	15.0%	None
♦	◊	17.5%	None
●	⊙	22.6%	W = 8.6%

$\frac{L}{d_D} = 9.0$ $\frac{A_D}{A_e} = 1.190$

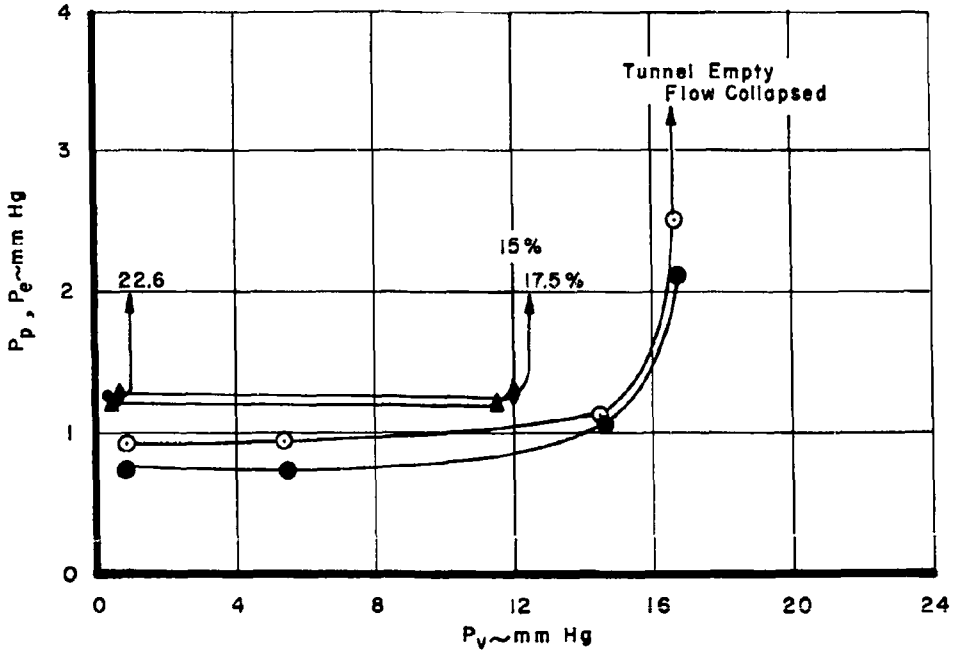

Figure 18. Vacuum Pump Inlet Pressure Effects - Diffuser V, Short Sting

TEST CONDITIONS			
P_{D_e}	P_D	Model Size	Minimum Plenum Pumping Required
●	⊙	None	None
▲	△	15.0%	None
◆	◇	17.5%	None
•	⊙	22.6%	W = 8.6%

$\frac{L}{d_D} = 9.0$ $\frac{A_D}{A_e} = 1.190$

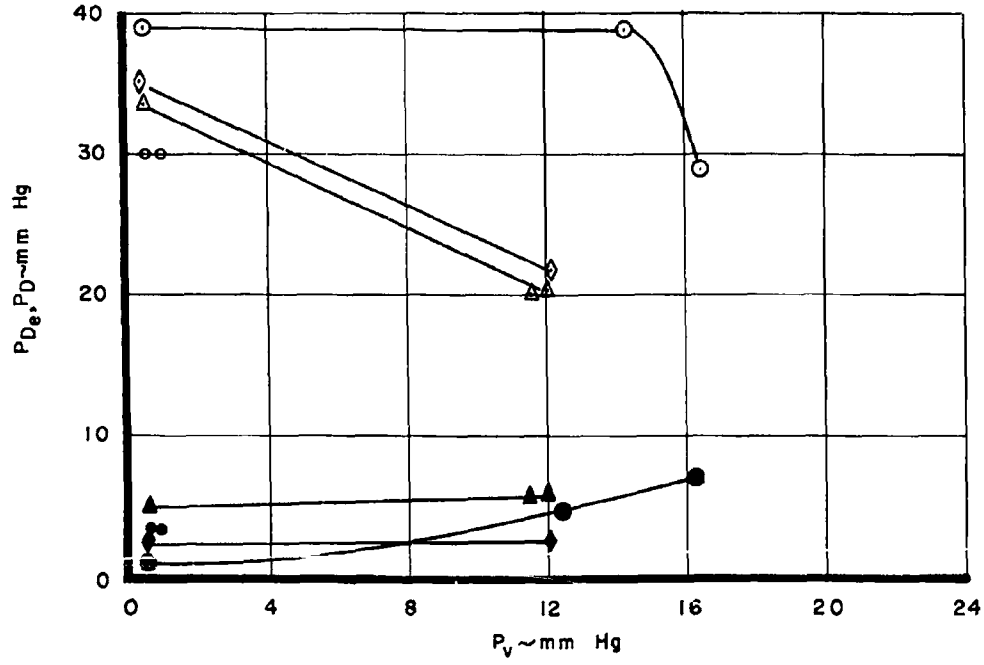

Figure 18. (Cont'd)

TEST CONDITIONS			
P_p	P_e	Model Size	Minimum Plenum Pumping Required
●	⊙	None	None
▲	△	12.9%	None
♦	◇	22.6%	None
◙	◎	24.2%	None
■	◎	27.3%	W = 4.6%
◤	◸	28.9%	W = 8.6%

$$\frac{L}{d_D} = 9.0 \qquad \frac{A_D}{A_e} = 1.450$$

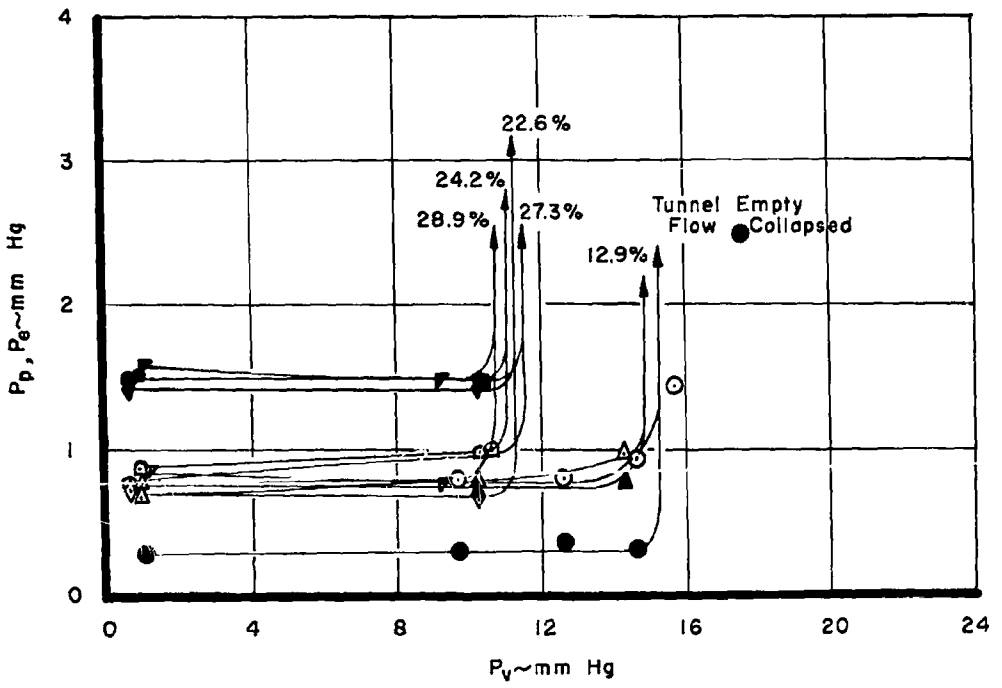

Figure 19. Vacuum Pump Inlet Pressure Effects - Diffuser VI, Long Sting

TEST CONDITIONS			
P_{D_e}	P_D	Model	Minimum Plenum Pumping Required
●	⊙	None	None
▲	△	12.9%	None
♦	◇	22.6%	None
■	⊡	24.2%	None
■	⊡	27.3%	W = 4.6%
◤	◸	28.9%	W = 8.6%

$\frac{L}{d_D} = 9.0$ $\frac{A_D}{A_e} = 1.450$

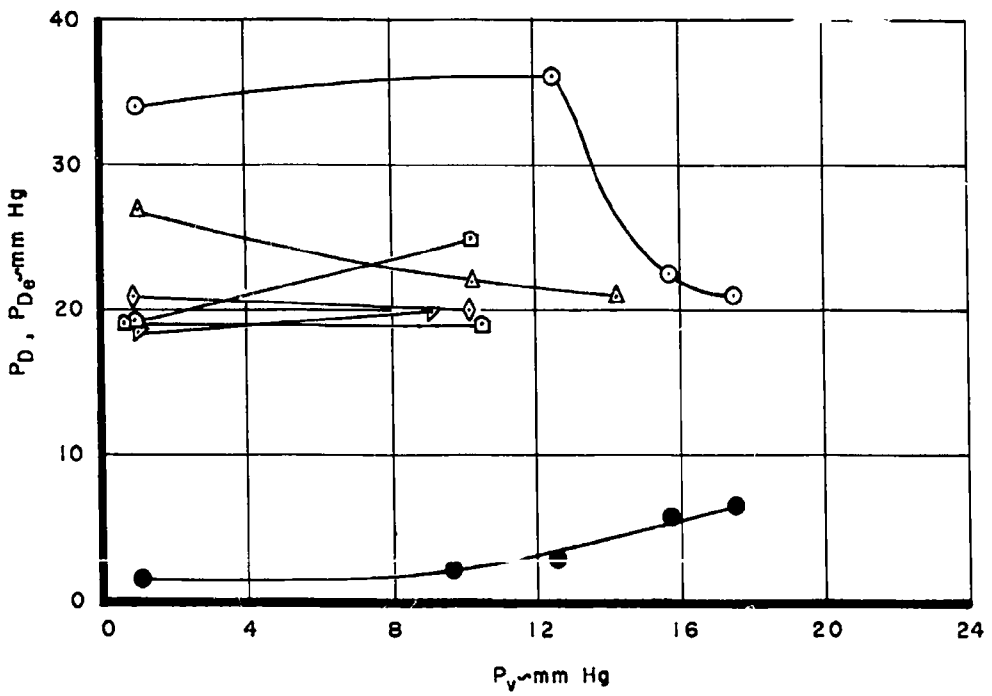

Figure 19. (Cont' d)

TEST CONDITIONS			
P_p	P_e	Model Size	Minimum Plenum Pumping Required
●	⊙	None	None
◆	◇	8.9%	None
◣	◺	15.0%	None
◆	◇	22.6%	None
◢	◿	25.7%	W = 2.0%
◙	◙	27.3%	W = 2.8%
◤	◸	28.9%	W = 8.6%

$\frac{L}{d_D} = 9.0$ $\qquad$ $\frac{A_D}{A_e} = 1.450$

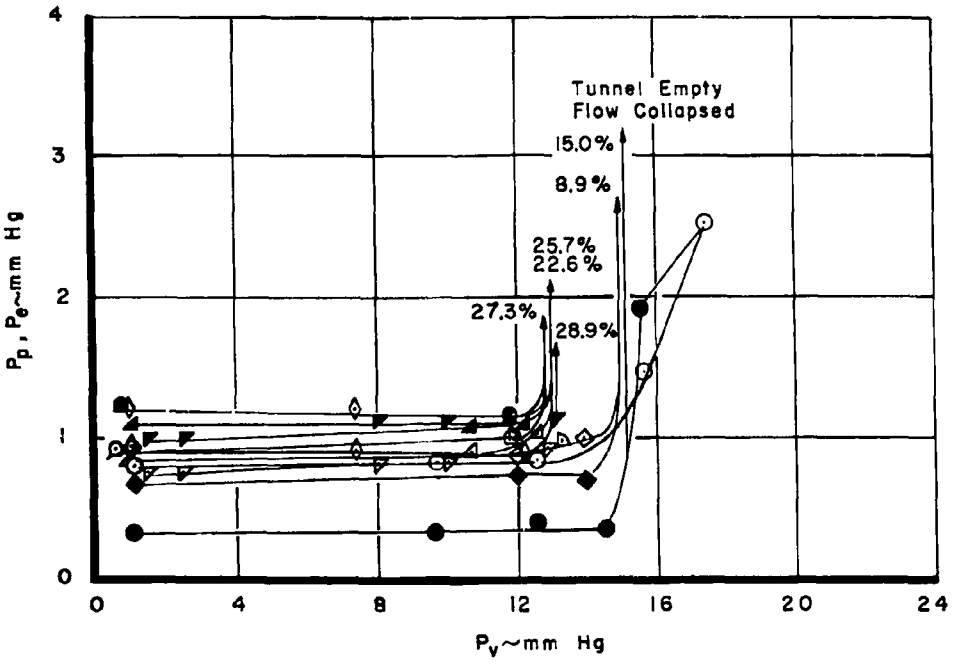

Figure 20. Vacuum Pump Inlet Pressure Effects - Diffuser VI, Short Sting

TEST CONDITIONS			
P_{D_e}	P_D	Model Size	Minimum Plenum Pumping Required
●	⊙	None	None
◆	◇	8.9%	None
◣	◺	15.0%	None
◆	◇	22.6%	None
◢	◭	25.7%	W = 2.0%
■	◻	27.3%	W = 2.8%
◤	◸	28.9%	W = 8.6%

$\frac{L}{dD} = 9.0$ $\frac{A_D}{A_e} = 1.45$

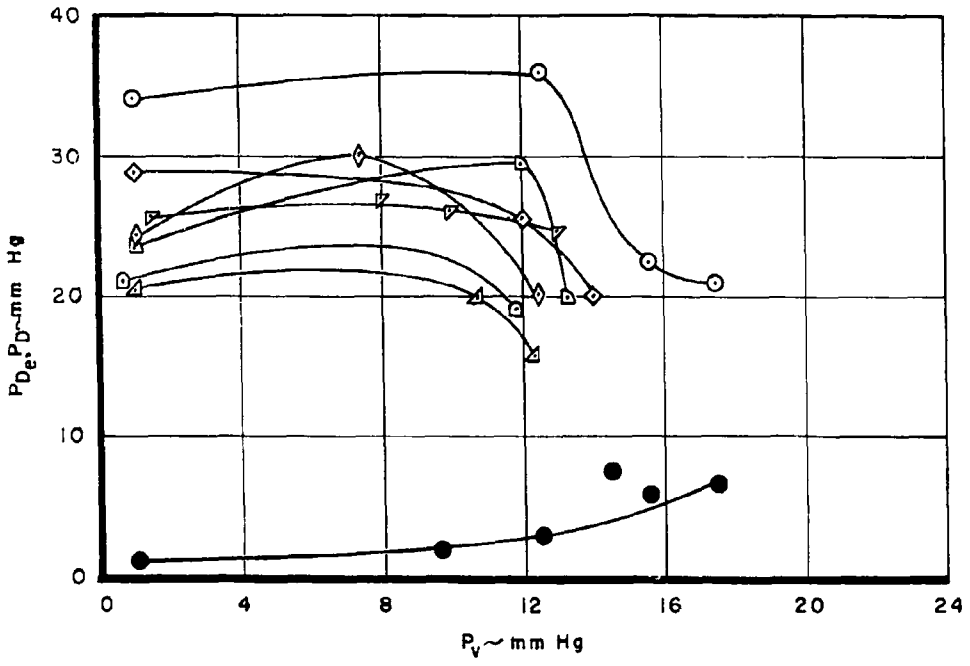

Figure 20. (Cont'd)

TEST CONDITIONS			
P_p	P_e	Model Size	Minimum Plenum Pumping Required
●	⊙	None	None
▲	△	12.9%	None
◣	◺	15.0%	None
◣	◺	17.5%	None
◆	◈	20.1%	None
■	▣	24.2%	W = 8.8%
◢	◿	25.7%	W = 8.7%

$\frac{L}{d_D} = 15.0$ $\frac{A_D}{A_e} = 1.190$

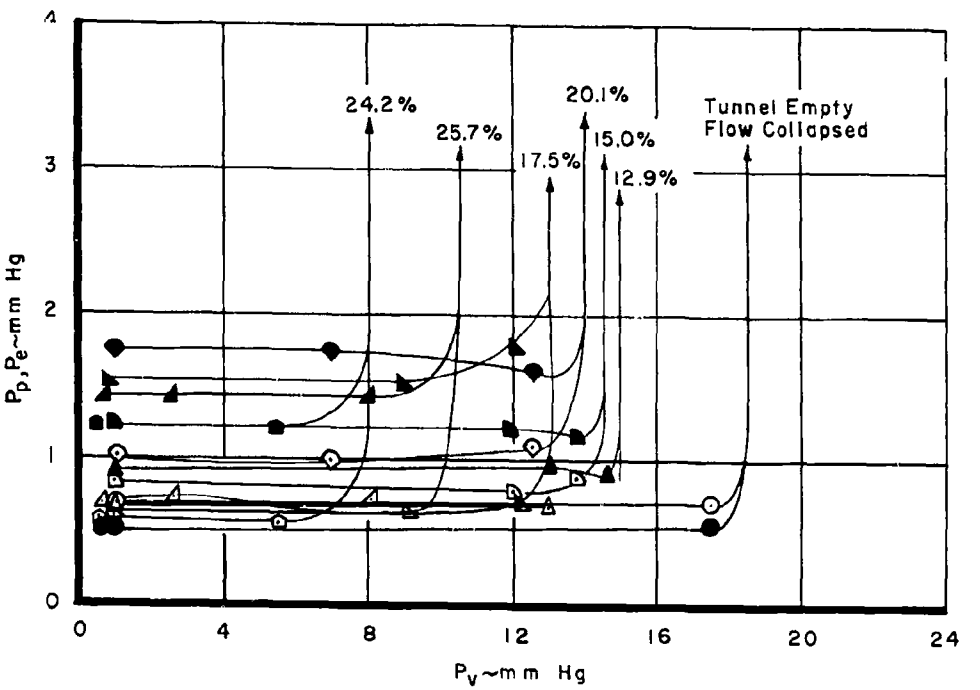

Figure 21. Vacuum Pump Inlet Pressure Effects - Diffuser VII, Long Sting

TEST CONDITIONS			
P_{D_e}	P_D	Model Size	Minimum Plenum Pumping Required
●	⊙	None	None
▲	◬	12.9%	None
◗	◺	15.0%	None
◣	◺	17.5%	None
●	⊙	20.1%	None
◗	◺	24.2%	W = 8.8%
◢	◬	25.7%	W = 8.7%

$\frac{L}{d_D} = 15.0$ $\frac{A_D}{A_e} = 1.190$

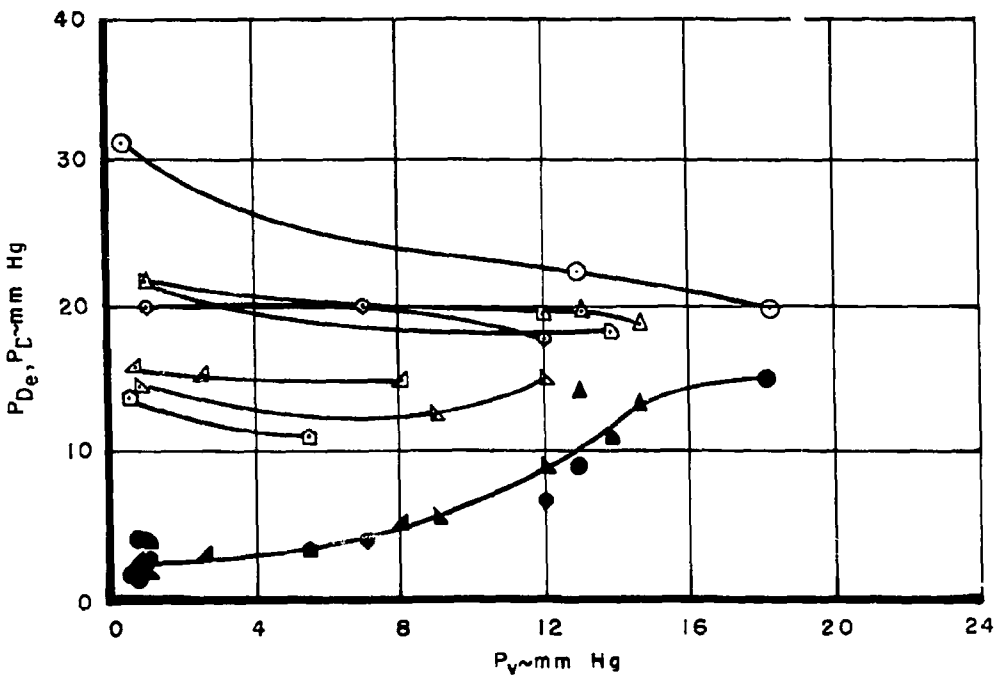

Figure 21. (Cont' d)

TEST CONDITIONS			
P_p	P_e	Model Size	Minimum Plenum Pumping Required
●	⊙	None	None
▲	△	12.9%	None
◣	◺	17.5%	None
♦	◊	22.6%	None
■	⌂	24.2%	None
◢	◿	25.7%	W = 5.0%

$\frac{L}{d_D} = 15.0$ $\qquad\qquad$ $\frac{A_D}{A_e} = 1.190$

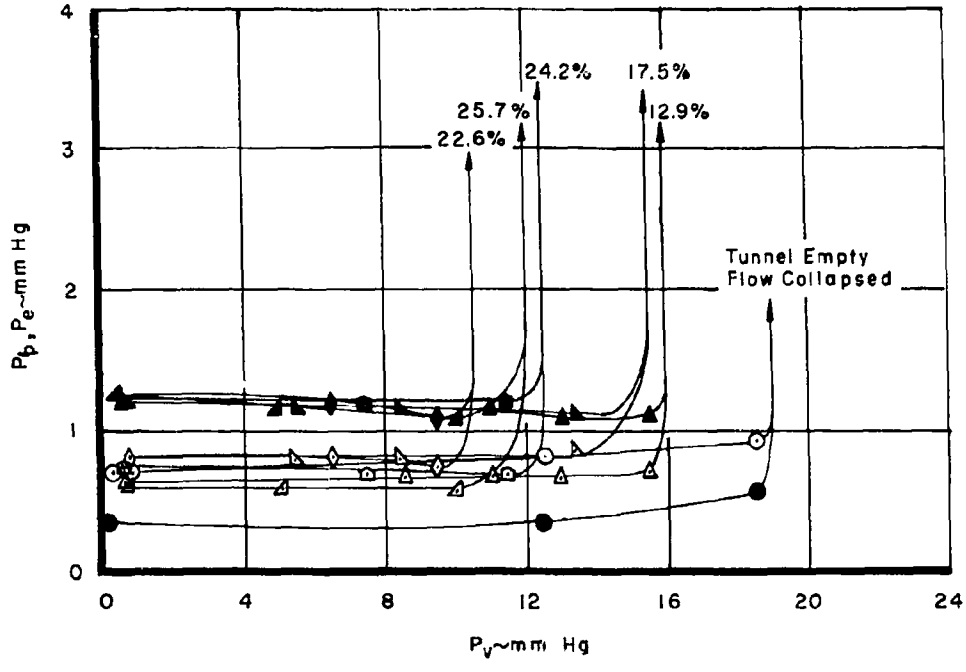

Figure 22. Vacuum Pump Inlet Pressure Effects - Diffuser VII, Short Sting

TEST CONDITIONS			
P_{D_e}	P_e	Model Size	Minimum Plenum Pumping Required
●	⊙	None	None
▲	△	12.9%	None
◣	◺	17.5%	None
♦	◇	22.6%	None
⬟	⬠	24.2%	None
◢	◿	25.7%	W = 5.0%

$\frac{L}{d_D} = 15.0$ $\frac{A_D}{A_e} = 1.190$

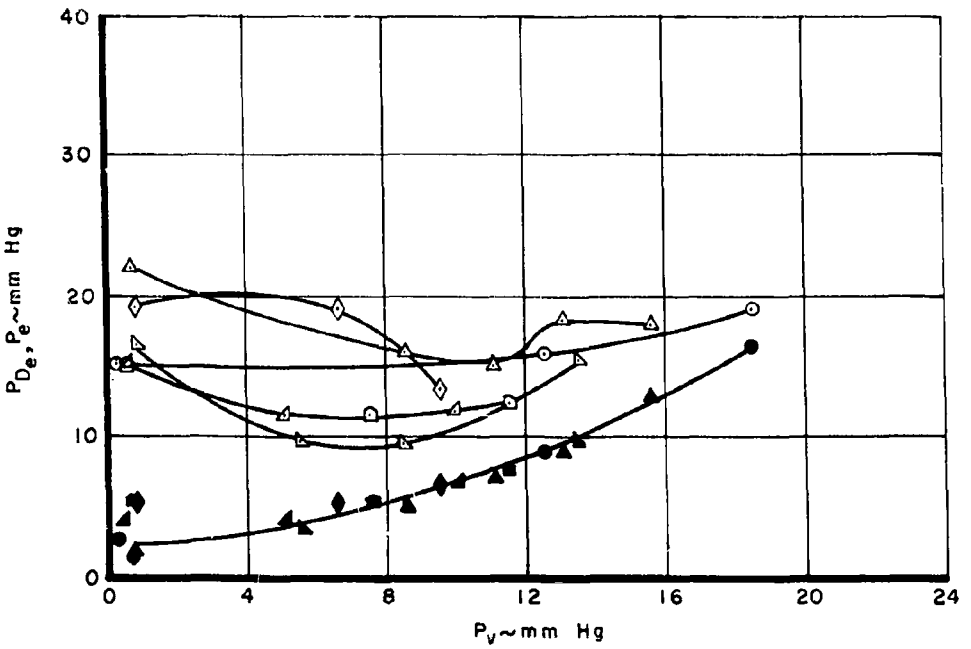

Figure 22. (Cont' d)

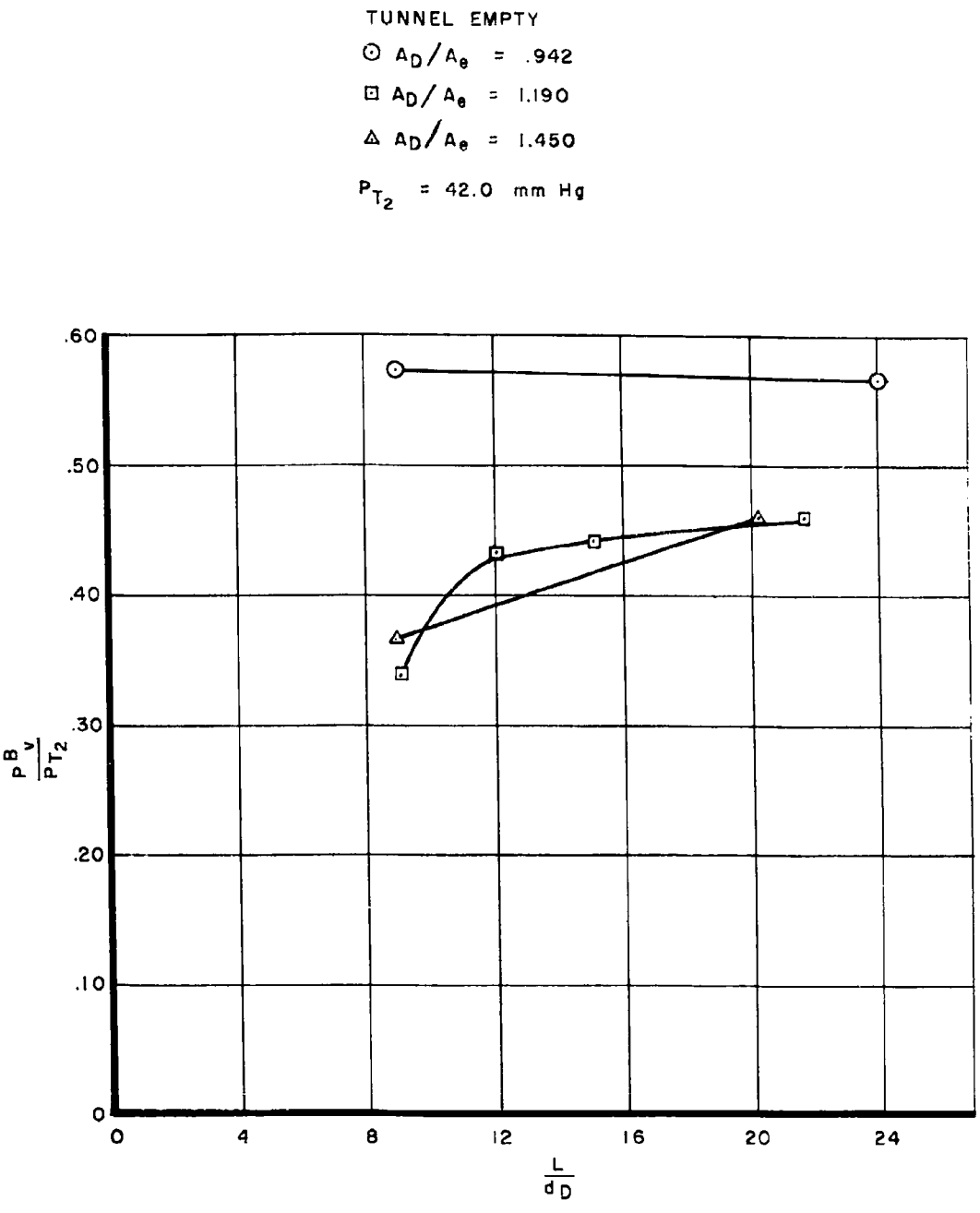

Figure 23. L/d_D Summary Curve - Diffuser Recovery Just Prior to Flow Collapsing, Tunnel Empty

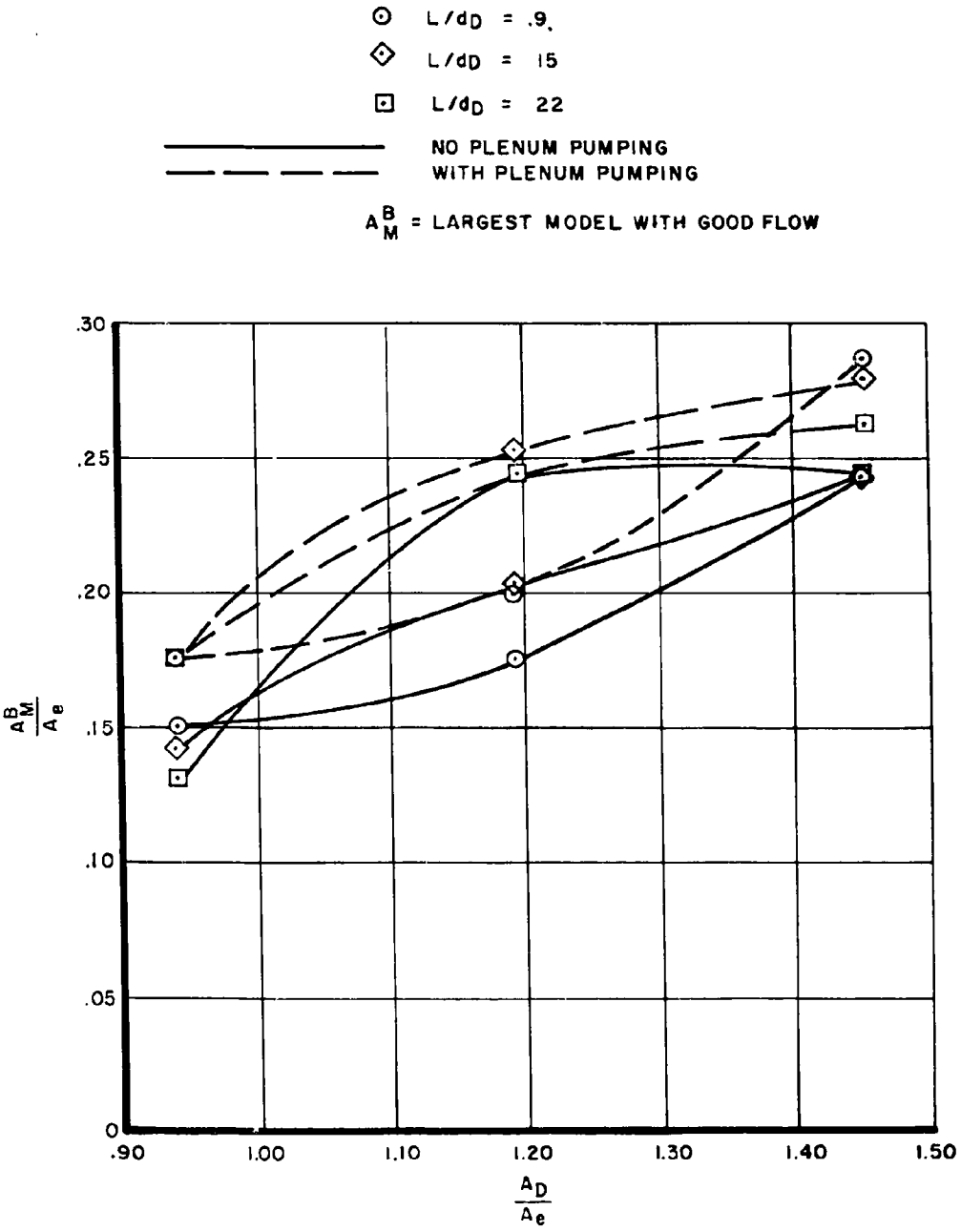

Figure 24. A_D/A_e Summary Curves for Blockage Models With Long Sting

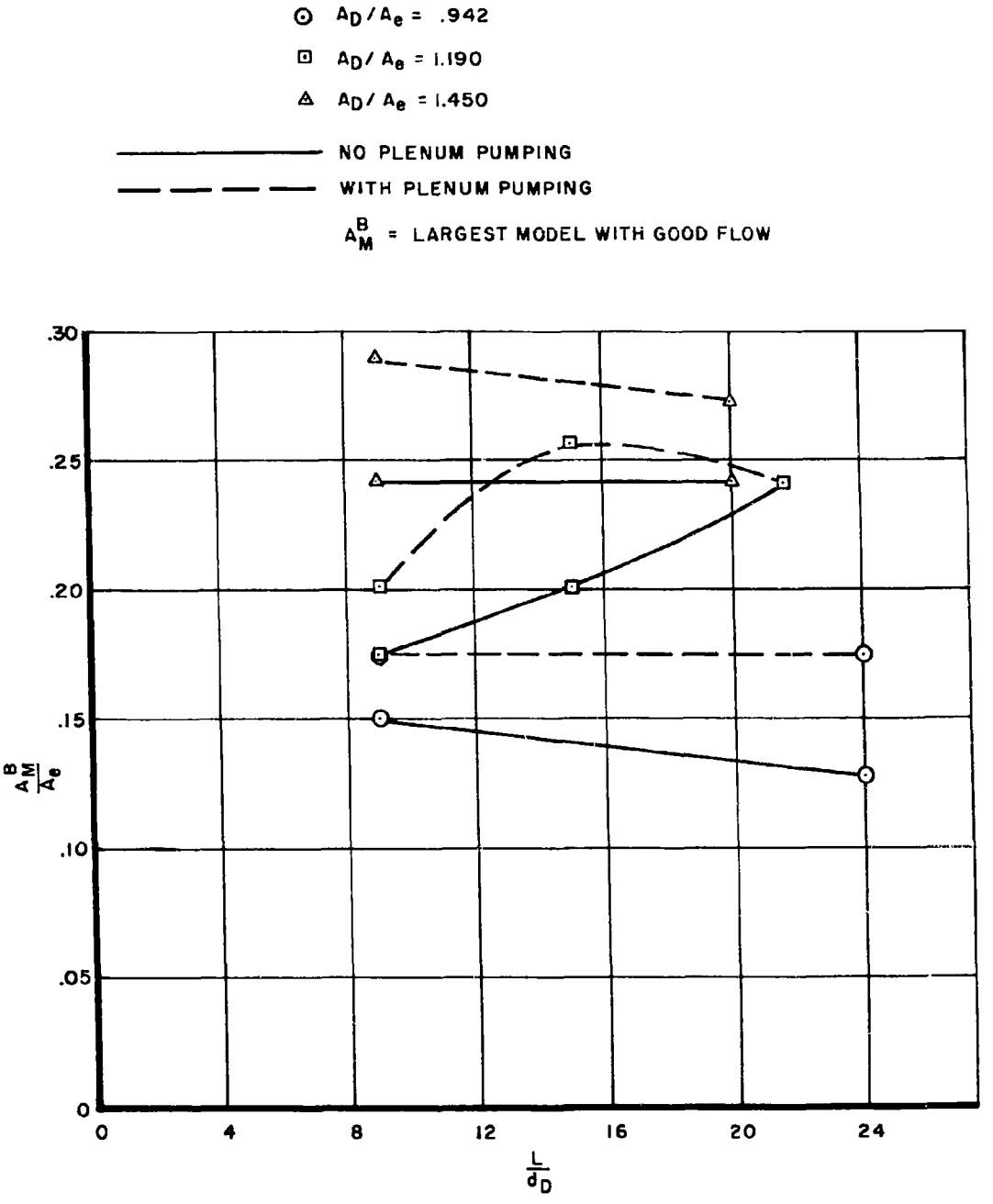

Figure 25. L/d_D Summary Curves for Blockage Models With Long Sting

TEST CONDITIONS		
P_p	P_e	Nominal Stagnation Enthalpy
●	⊙	3000 BTU/lb
■	⊡	4800 BTU/lb
◆	◇	6000 BTU/lb

$\frac{L}{d_D} = 12.0$ $\qquad\qquad$ $\frac{A_D}{A_e} = 1.19$

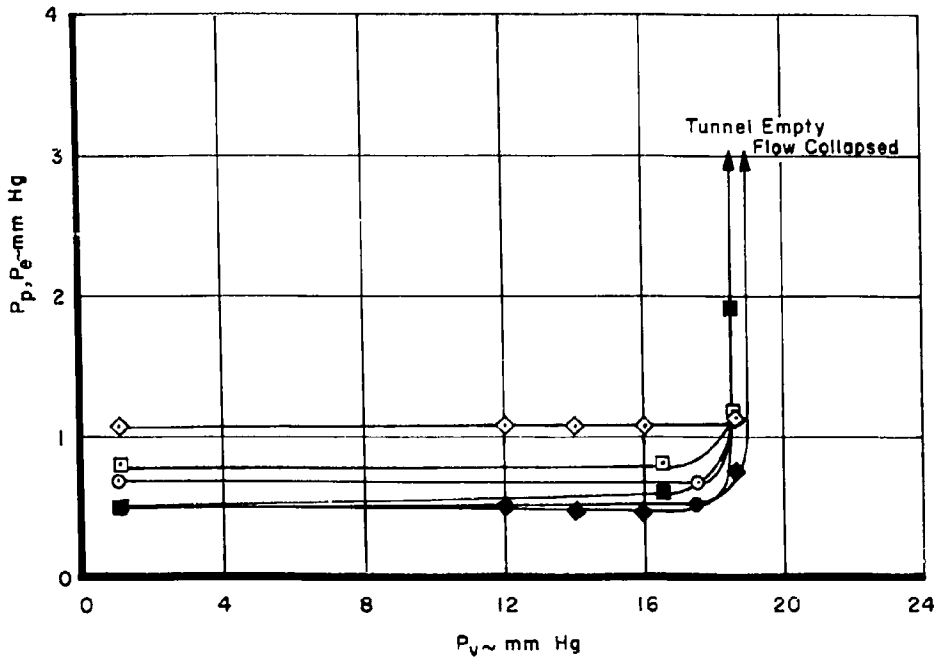

Figure 26. Vacuum Pump Inlet Pressure Effects for Various Total Enthalpies Diffuser VIII, No Models

TEST CONDITIONS		
P_{De}	P_D	Nominal Stagnation Enthalpy
●	⊙	3000 BTU/lb
■	⊡	4800 BTU/lb
◆	◇	6000 BTU/lb

$\frac{L}{d_D} = 12.0$ $\qquad\qquad$ $\frac{A_D}{A_e} = 1.19$

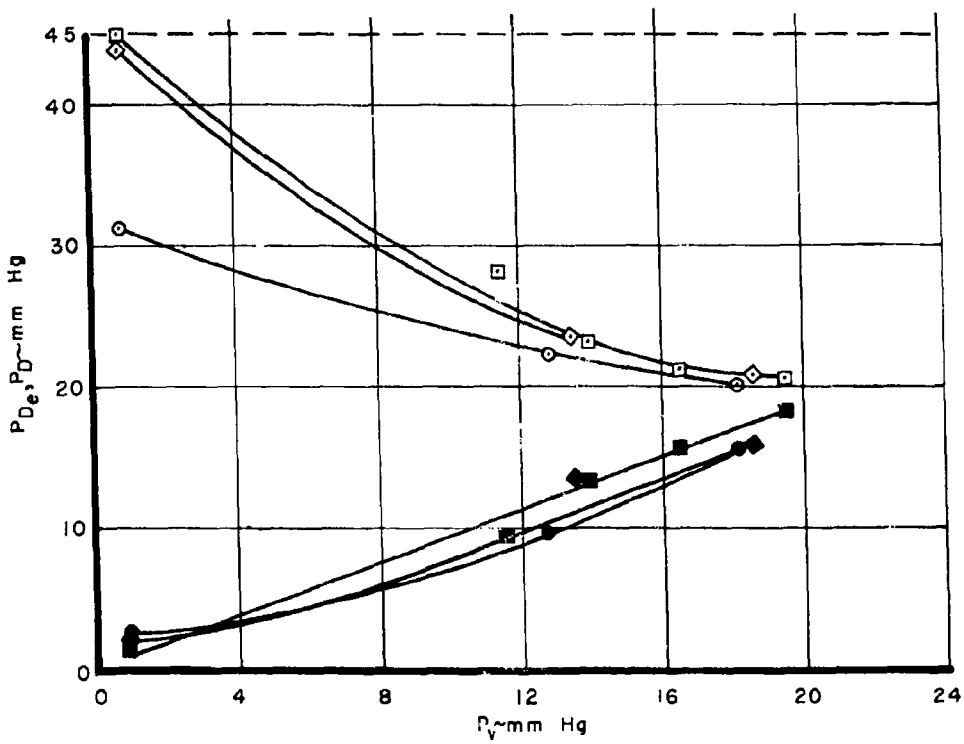

Figure 26. (Cont'd)

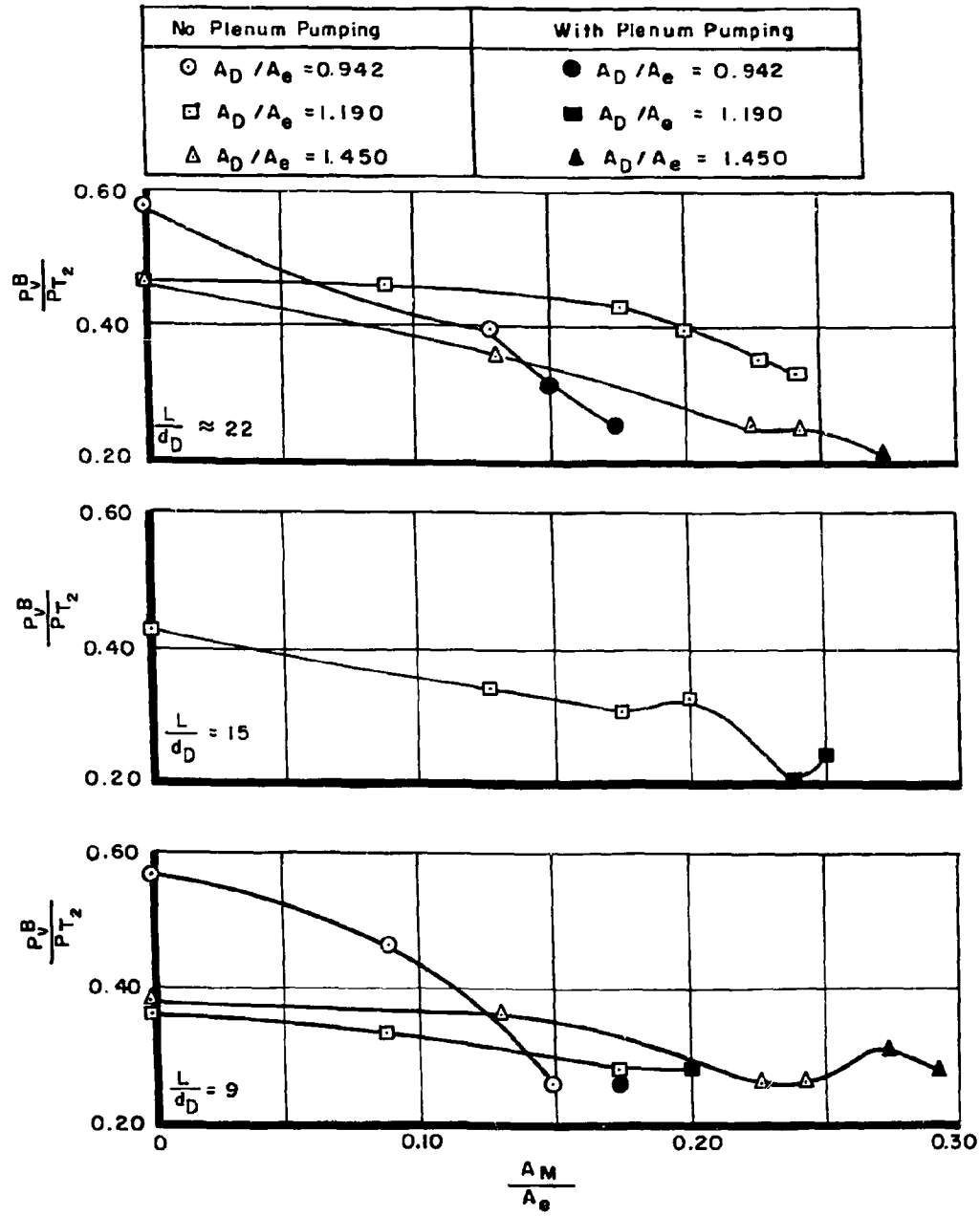

Figure 27. Diffuser Recovery With Various Blockage Models With and Without Plenum Pumping